CHARACTERIZATION OF INVASION PLASMID ANTIGEN B AND C (IpaB AND IpaC) TRANSLOCATOR COMPLEXES AND TRANSLOCATOR/CHAPERONE COMPLEXES OF *Shigella flexneri*

by

Christina Marie Terry

Submitted to the graduate degree program in Department of Molecular Biosciences and the Graduate Faculty of the University of Kansas in partial fulfillment for the requirements of the degree of Master of Arts

_____
Chair
Dr. William Picking

_____
Committee Member
Dr. Roberto DeGuzman

_____
Committee Member
Dr. Dean Stetler

_____
Date defended

Thesis committee for Christina Terry certifies that this is the approved Version of the following thesis:

CHARACTERIZATION OF INVASION PLASMID ANTIGEN B AND C (IpaB AND IpaC) TRANSLOCATOR COMPLEXES AND TRANSLOCATOR/CHAPERONE COMPLEXES OF *Shigella flexneri*

Committee

_____

Dr. William Picking, Chair

Dr. Roberto DeGuzman

Dr. Dean Stetler

Date approved April 23, 2008

ABSTRACT

Shigellosis, a severe form of bacillary dysentery, is primarily caused by the gram negative pathogen, *Shigella flexneri.* In order to elicit disease, the pathogen must pass through the digestive tract and induce its uptake by colonic epithelial cells. To facilitate this process, *S. flexneri* uses a type III secretion system (TTSS) to form a pore in host cell membranes and deliver translocator and effector proteins to the targeted host cells. Translocon pore formation is the responsibility of the invasion plasmid antigens IpaB and IpaC. Prior to their secretion, IpaB and IpaC are stored in the bacterial cytoplasm where they individually associate with the molecular chaperone IpgC. In this study, a variety of biophysical and molecular techniques were utilized to investigate the structural and functional characteristics of these proteins and the interactions of the translocator/chaperone and the translocator/translocator complexes.

ACKNOWLEDGEMENTS

I would like to thank Dr. William Picking and Dr. Wendy Picking for allowing me to work in their laboratory. This work would not have been possible without the resources and guidance that they have provided over the past two years. I consider myself lucky to have worked for two supportive mentors that have fostered such an enjoyable lab environment. It is a rare find to work in a place where you thoroughly enjoy going to work. I would also like to thank all of my fellow lab mates who all, at one time or another, have either provided advice, support, technical assistance or knowledge that proved to be invaluable over the course of my time at the University of Kansas, especially Lingling Zhang, Marianela Espina, Andrew Olive and Nathan Smith.

Additionally, this work would not be complete without the aid and expertise from the Middaugh lab in the pharmaceutical chemistry department, particularly Aaron Markham and Brooke Barrett.

I would also like to thank my committee members Dr. Roberto DeGuzman and Dr. Dean Stetler for taking the time to read this thesis and offer suggestions and comments to improve this work.

Finally, I would like to thank my family, who has been with me through all the difficult times, when the lab work could not just stay on campus. My parents have always been supportive of my decisions throughout life, no matter what. Most of all I want to thank my husband, Luke. His patience and support has always been unwavering.

TABLE OF CONTENTS

LIST OF FIGURES AND TABLES

CHAPTER 1

Introduction

Diarrheal diseases affect billions of people worldwide each year. Shigellosis, a severe form of bacillary dysentery, is caused by the gram negative bacillus, *Shigella flexneri* and its close *Shigella* relatives. Although, most cases of shigellosis are due to endemic infections by *S. flexneri* in developing regions, approximately 20,000 cases are reported in the US each year and this rate of incidence may be significantly under-estimated. Additionally, increasing antibiotic resistance has compounded the need for research into vaccine development for this pathogen.

Historical Perspective

The etiological agent of bacillary dysentery was first described by Kiyoshi Shiga during the 1897 *sekiri* outbreaks in Japan. During the observation of 36 dysentery patients, bacilli were isolated from the stool of the patients and found to cause similar symptoms in dogs when introduced orally (Shiga 1897). In subsequent years, Shiga continued to characterize the organism and eventually named it *Bacillus dysenteriae* (Shiga, 1897).

In the years following Shiga's initial observation of *Bacillus dysenteriae*, many investigators worked to characterize the organism. Several investigators began to report and characterize organisms that demonstrated similar disease and that were morphologically and biochemically comparable to the organism described by Shiga

(Flexner 1900, Kruse 1900). By 1952, the Congress of the International Association of Microbiologists (*Shigella* Commission) officially adopted the current genetic name *Shigella*, in honor of Shiga's work with the organism. The genus *Shigella* belongs to the family Enterobacteriaceae and has grown to include four species, *S. boydi, S. dysenteriae, S. flexneri* and *S. sonnei.*

After the 1950's, emphasis grew on defining and characterizing the mechanism of virulence in *Shigella*. Although shigellosis is limited in host range to humans and other high primates, animal models began to emerge in the 1950's and 1960's beginning with the adaptation of *Shigella* infection to the corneal epithelium of guinea pigs (Sereńy test) (Sereńy 1957). Soon after, it was demonstrated that *Shigella* could be grown in cultured mammalian cells (Gerber and Watkins 1961). More recently, high doses have been found to induce pneumonia and diarrhea in rats if introduced nasally or rectally, respectively (Mallet *et al.,* 1993) (Kamgang *et al.,* 2005).

Until 1964, it was believed that the pathogenicity of *Shigella* was due primarily to the release of bacterial toxins while the pathogen adhered to the surface of intestinal epithelial cells (Watkins, 1960). Work by LaBrec *et al*. demonstrated that feeding virulent strains *S. flexneri* to guinea pigs resulted in the ulceration, and penetration of the epithelial cells of the colon and lamina propia, establishing that invasion of the colonic epithelium was an essential aspect of the disease (LaBrec *et al*., 1964).

The genetic basis for *Shigella* pathogenesis was not determined until the 1980's. Sansonetti and colleagues discovered that *S. sonnei* and *S. flexneri* virulence was dependent upon the presence of a large plasmid. Loss of this plasmid resulted in the inability of the organism to invade mammalian cells in culture or evoke keratoconjuctivitis in guinea pigs (Sansonetti 1981, Sansonetti 1982). Eventually, it was established that all *Shigella* species possess a large (200 kDa), low-copy number virulence plasmid containing genes essential for cellular invasion. Much of the current work on *Shigella* continues to work toward characterizing and understanding the genes and proteins encoded on this plasmid.

Epidemiology and Pathology

Bacillary dysentery, or shigellosis, is primarily a disease of humans and other higher primates which is largely limited to the intestinal mucosa. Symptoms typical of shigellosis are watery diarrhea with mucus, fever, malaise, and abdominal cramping. The severity and range of symptoms may be dependent upon the number of organisms ingested and species. Disease can be further complicated by septicemia, hypoglycemia, bacteremia, dehydration, uremic and hemolytic syndrome and toxic megacolon (Phalipon and Sansonetti, 2007).

Shigella is responsible for more than 150 million cases of bacillary dysentery worldwide each year, which ultimately results in more than one million deaths (Hueck 1998) (Kotloff et al., 1999) (Venkatesan 2001). The incidence of fatality is higher in children under the age of five due to complications that result from

dehydration and malnutrition. *S. flexneri* is the most common species encountered in endemic areas, while *S. sonnei* is more prevalent in industrialized nations.

Shigella infection is acquired via the fecal-oral route and epidemics of the organism are clearly associated with poor hygienic practices and contaminated food and water sources (DuPont 1989). In the United States, outbreaks are generally associated with child care facilities, community homes and prisons. Additionally, homosexual men are more susceptible to shigellosis and reoccurring cases have been found to cause complications when associated with AIDS (Blesser *et al.,* 1989). In developing nations, crowding and sewage contamination of water supplies commonly lead to *Shigella* outbreaks in the general population. Most often infections are associated with *S. flexneri*, but epidemic outbreaks are generally traceable to *S. dysenteriae*. The latter organism is most often associated with fatal cases of shigellosis due to the synthesis of a potent exotoxin (Shiga toxin) (O'Brien *et al.,* 1980).

The organism enters the host orally and travels through the digestive system until it reaches the large intestine. Invasion of the intestinal epithelium by *Shigella* cannot occur via the apical side of the mucosal epithelial cells, so the organism must first make its way to the basal face of the epithelium to initiate invasion. Thus, upon reaching the large intestine, *Shigella* is taken up in vacuoles by microfold cells (M cells) in the colon (Owen 1986) (Wasset 1989). The organism escapes from the vacuole and eventually travels to underlying macrophages that are associated with M cell-associated lymphoid follicles (Sansonetti *et al.,* 1996). The organism is taken up

by the phagocyte, which then induces apoptosis which results in the escape of the pathogen to the basal side of the colonic epithelium. Death of the macrophage results in the release of IL-1β. This proinflammatory cytokine eventually results in the recruitment of PMN cells to site of infection and the onset of inflammation (Zychlinsky *et al.,* 1994) (Sansonetti *et al.,* 2000). Meanwhile, the bacteria induce their own uptake into colonic epithelial cells and spread laterally through the cells of the epithelium by a process known as actin based motility (ABM) (Mounier 1992). Ultimately, it is the cells of the host's immune system that cause inflammation and ulceration of the mucosa to the colon and the symptoms associated with shigellosis (Wassef 1989) (Islam 1997).

The pathogen

Shigella belongs to the tribe *Escherichieae*, which are members of the family Enterobacteriaceae. Like other pathogens of this family, *Shigella* is a gram-negative gastrointestinal pathogen, primarily responsible for disease in humans and primates. Like other organisms belonging to this family, *Shigella* is facultatively anaerobic, oxidase negative and possesses the abilities to reduce nitrate and ferment glucose. Differentiation among the species can be accomplished biochemically by testing for ornithine decarboxylation and mannitol and xylose fermentation (Kreig, 1984). Additionally, species identification can be determined serologically, as all species possess species-specific O-antigen components (Kreig, 1984).

Shigellosis is highly contagious and infectious, requiring relatively few organisms to elicit disease (10-100 organisms) (DuPont, 1989). Infection is generally associated with poor sanitation and outbreaks are usually linked to a contaminated food or water source. The disease is generally self limiting (symptoms usually last 5-7 days) and is routinely treated with oral antibiotics (Hueck, 1998). Currently, oral antibiotics are the preferable means of treatment; however, emerging antibiotic resistance is limiting the number of drugs available for the treatment of shigellosis. Strains resistant to tetracycline, sulfonamides, ampicillin and trimethoprim-sulfamethoxazole have been found worldwide (Hueck, 1998).

Genetic Determinants of Virulence

The virulence of *Shigella* is dependent upon a number of genes located on pathogenicity islands found in both the chromosome and on a large virulence plasmid found in all *Shigella* species. These pathogenicity islands encode a number of virulence functions including antibiotic resistance, iron acquisition, proteases and cellular invasion (Schroeder and Hilbi, 2008).

Potentially the most vital component of *Shigella's* virulence arsenal is a large virulence plasmid that contains the genes required for cellular invasion. These virulence plasmids range in size among species, but average in size at about 200 kb and they have been found to possess approximately 100 genes (Sansonetti 1985) (Yoshikawa 1988). The virulence plasmid is primarily responsible for the uptake and dissemination of the bacteria throughout the cells of the colonic epithelium

(Wantanbe 1989). The means for this uptake is via a type three secretion system (TTSS) which is encoded in a 31-kb "entry region" of the virulence plasmid. Genes outside the "entry region" encode proteins for virulence factors that play roles after invasion of the host cell (Sansonetti 1985) (Yoshikawa 1988). It has been determined that loss of this plasmid results in a loss in the ability to cause disease (Yoshikawa 1986). Additionally, transfer of the virulence plasmid into avirulent lab strains of *E. coli* confers an invasive phenotype to these non-pathogens (Formal 1982).

Genes of the "entry region" fall into one of four categories based upon function. The first category is comprised of proteins secreted by the TTSA. These primarily consist of the *ipa* (invasion plasmid antigen) genes which are primarily effector and/or translocator proteins directly responsible for inducing cytoskeletal rearrangements, membrane ruffling and pathogen uptake. Group two comprises genes that make up the type III secretion apparatus. These consist of the *mxi* (membrane expression of *ipa* proteins) and the *spa* (surface presentation of *ipa* antigens) genes. Many of these proteins are polymers that assemble to form the structural components of the TTSS apparatus including the basal body and the needle. The third category is reserved for the transcriptional activators of the TTSS genes in the "entry region," such as *mixE* and *virB*. Lastly, there are the molecular chaperones of the TTSS that help to maintain effector proteins while they are in the bacterial cytoplasm (Schroeder and Hilbi, 2008).

The Type III Secretion System

The TTSS is utilized by *Shigella* to invade the epithelial cells of the human colon. It accomplishes this through an arsenal of proteins designed to penetrate and manipulate the targeted host cell. Acting as a molecular syringe, the TTSA injects effector proteins into the host cell. Once inside the cell, the effector proteins interact with the host cell's signaling molecules to induce cytoskeletal rearrangements and promote uptake of the bacterium (Cornelis, 2006).

The basal body of the TTSA is a seven-ringed structure that spans the inner and outer membrane of the bacterium. From the basal body extends the needle of the apparatus. The needle protrudes from the outer membrane into the environment surrounding the bacterium. Within the cytoplasm, at the bottom of the basal body, lies an ATPase implicated in protein unfolding, chaperone release and transmembrane transport of substrate proteins (Figure 1.1) (Blocker *et al.,* 2001).

The Ipas

Effector proteins of the TTSS are utilized by *Shigella* to gain entry into and hijack the cytoskeletal proteins of the target cell to induce uptake of the bacterium. Beyond the polymer base of MxiH, IpaD sits at the tip of the needle apparatus. Upon host cell contact or conditions that mimic host cell contact, additional effector proteins are secreted by the TTSA. In the lab, it has been demonstrated that the addition of the small amphipathic dyes Congo red, brilliant orange or Evans blue can induce secretion of TTSS effector proteins in the absence of host cell contact (Parsot

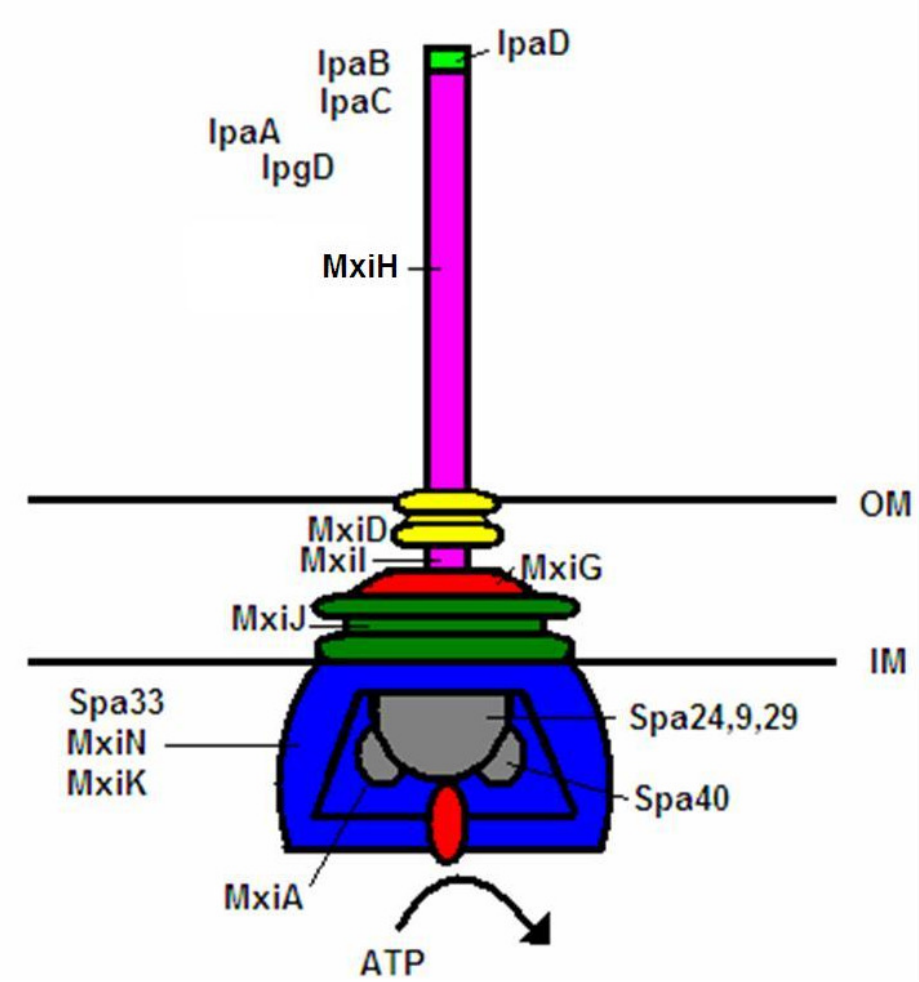

Figure 1.1 Schematic of the proteins of the type III secretion apparatus of *Shigella flexneri.*

et al., 1995) (Bahrani *et al.,* 1997). Additionally, serum has been demonstrated to have similar effects on the secretion system, though it is unclear how this latter mechanism works (Parsot *et al.,* 1995) (Bahrani *et al.,* 1997).

IpaD has been shown by Espina *et al.* to localize at the tip of the TTSA needle capping the MxiH polymers (Espina *et al.,* 2006). IpaD also possesses some form regulator function since *ipaD* null mutants are not able to invade and in overnight cultures they hypersecrete the TTSS effector proteins into the extracellular environment (Menard *et al.,* 1994b) (Picking *et al.,* 2005). Work in progress by others in our group has demonstrated that the presence of bile salts (specifically deoxycholate) can induce IpaB to be secreted and sit at the tip of the needle after IpaD. This has been proposed as a priming step, preparing the needle for host cell interaction via the cholesterol binding function of IpaB (Olive *et al.,* 2007).

After IpaD, IpaB is recruited to the tip of the needle (Olive *et al.,* 2007). Prior to its secretion by *S. flexneri*, however, IpaB is bound by the molecular chaperone, IpgC, within the bacterial cytoplasm. This association prevents IpaB degradation, aggregation and it is believed to maintain IpaB in a pre-secretion state for its subsequent passage through the TTSA needle (Menard *et al.,* 1994a) (Page *et al.,* 1999). Before *S. flexneri* is able to invade epithelial cells, it must escape from its host macrophage. IpaB appears to be the protein responsible for inducing phagocyte apoptosis by inducing a caspase-1 dependent pathway (Zychlinsky 1998). Like IpaD, IpaB appears to control effector regulation, since *ipaB* null mutants are also non-invasive and hypersecrete effectors into overnight culture supernatant fractions

(Menard *et al.,* 1994b). Along with IpaC, IpaB is a component of the translocon, a pore like structure that is inserted into the host cell's cytoplasmic membrane while maintaining contact with the TTSA needle component via IpaD. This allows subsequent effector proteins to gain access to the cytoplasm of the target cell.

IpaB secretion is followed by the secretion of IpaC. Prior to its secretion, IpaC also binds to IpgC in the bacterial cytoplasm, serving the same purpose as formation of the IpaB/IpgC complex (Menard *et al.,* 1994a) (Page *et al.,* 1999) . In addition to forming the translocon, IpaC has been implicated in cell signaling within the host cell. IpaC has been proposed to interact with a small Rho-family GTPase called Cdc42 leading to the formation of filopodial extensions (Tran Van Nheiu and Sansonetti, 1999). Although it has been shown that IpaC can nucleate actin, its interaction with Cdc42 remains largely unknown (Kueltzo *et al.,* 2003). IpaC induced membrane extensions gradually envelope the bacterium and lead to the formation of a phagosomal vacuole around the pathogen (Tran Van Nheiu *et al.*, 1999)

Upon formation of the translocon, *Shigella* transfers additional TTSS effector proteins into the host cell to induce cytoskeletal rearrangement and phagocytosis (Menard *et al.,* 1994b) (Watarai *et al.,* 1995) (Menard *et al.,* 1996) (Blocker *et al.,* 1999). Though the exact pathway through which these interactions occur have yet to be elucidated. IpaA, IpaB1, IpaB2, IpaC and IpgD are the most studied of these effector proteins responsible for inducing phagocytosis by the host eukaryotic cell. IpaA possess the ability to depolymerize actin, while IpaB1 and IpaB2, appear to

mimic RhoG and RhoA, respectively, inducing the formation of lamellipodia and actin stress fibers (Alto *et al.,* 2006) (Handa *et al.*, 2007) Finally, IpgD has been described as a phosphoinositide 4-phosphatase, which facilitates the hydrolysis of phosphatidylinositol-4,5-biphosphate [PtdIns(4,5)P_2], resulting in the dissociation of the cytoskeleton from the plasma membrane (Hilbi, 2006) (Niebuhr *et al.,* 2002).

Escape into the cell cytoplasm

In order to replicate and spread throughout the colonic epithelium, *Shigella* must escape the phagosome and gain access to the cytoplasm of the host cell. Proteins required for phagosomal escape appear to be independent of those required for bacterial uptake. In *S. flexneri* strains in which the 31-kb entry region is deleted, and complemented with the *Salmonella enterica* serovar Typhimurum *Salmonella* pathogenicity island -1 (SPI-1), invasiveness and phagosomal escape are restored (Paetzold *et al.*, 2007). These results would be expected as many of the genes in SPI-1 are homologous to those found on the *S. flexneri* virulence plasmid. Unlike, *S. flexneri*, *S. typhimurium* does not require escape from the phagosome to replicate (Takeuchi, 1967) (Sansonetti *et al,* 1986). In *S. flexneri* strains lacking the entire virulence plasmid, but containing SPI-1 are capable of invasion, but cannot escape the phagosome, suggesting genes vital to *S. flexneri* phagosomal escape lie outside of the 31-kb entry region of the virulence plasmid (Paetzold *et al.,* 2007).

Once *Shigella* has escaped the phagosome, it can spread laterally across the colonic epithelium. Though *Shigella* is non-motile, it possesses the ability to move

through the host cell cytoplasm via actin-based motility. IcsA (intracelluar spread) localizes at one pole of the bacterium and mediates actin polymerization. Through the aid of IcsP and PhoN2, IcsA interacts with host cell N-WASP and Arp2/Arp3, to nucleate actin and move the bacterium through the cytoplasm. At the opposite pole of the bacterium, VirA works to depolymerize α-tubulin to create a path for *Shigella* to move through (Schroeder and Hilbi, 2008).

Eventually, the bacterium makes its way to the tight junctions between the host epithelial cells. Here it enters the neighboring cell to reside in a double-membraned vacuole. This vacuole is lysed and the pathogen escapes into the cytoplasm of the neighboring cell. The bacterium will then replicate and continue to spread laterally across the epithelium (Parsot, 1994).

Research foci

The research presented here addresses the interactions of IpaB and IpaC with one another and with the chaperone IpgC. Most research in the field has focused on characterizing these proteins individually rather than in conjunction with their partner proteins. Structure function analyses of both IpaB and IpaC have helped to identify key regions and their associated functions. Data here extend and complement these structure-function analyses and more intimately characterize key regions within IpaC.

Because these proteins spend their functional lives in complexes with either a chaperone or within the translocon, it is also important to investigate the influence that these complexes have on protein structure and function. IpaBC translocon formation is vital to *Shigella* invasion. In the absence of the translocon, the pathogen

is no longer invasive and unable to elicit disease in the host. Though it is widely accepted that IpaB and IpaC form a pore that inserts into the host cell membrane, characterization of this complex has been relatively neglected. Using various biophysical and molecular methods, we have characterized some of the structural aspects of the IpaBC pore and how these proteins work to interact with artificial membranes (Chapter 4).

In addition, little research has been devoted to characterizing the influence of IpgC binding upon the solution properties of IpaB or IpaC. Recently, we utilized tryptophan scanning mutagenesis to determine the polarity of specific microenvironments within IpaC and how those environments are influenced by IpgC binding. Chapter 3 addresses the IpaC/IpgC interaction. Results from this study have suggested that IpgC binding has a strong influence on key regions of the N- and C-termini of IpaC (Birket *et al.*, 2007). Here, we have begun to use the same techniques to identify and characterize residues within IpaB influenced by IpgC binding (Chapter 5).

CHAPTER 2
Materials and Methods

Reagents and Buffers

10 X Buffer Z
2.42 g Tris
2.92 g $NaCl_2$
100 ml diH_2O

20 mM Citrate Phosphate Buffer, pH 7
Solution 1(0.4 M Sodium phosphate dibasic)
56.78 g Na_2HPO_2, anhydrous
1.00 L diH_2O
Solution 2 (0.4 M Citric Acid)
76.85 g $C_6H_8O_7$, anhydrous
1.00 L diH_2O

(90 ml Solution 1) + (10 ml of Solution 2) + (1900 ml diH_2O)

Coomassie Blue Protein Gel Stain
250 ml methanol
1.25 g Coomassie brilliant blue
75 ml acetic acid
175 ml diH_2O

Congo Red Agar (CR)
40.0 g TSA
4.00 g agar
0.300 g Congo Red
1.00 L diH_2O

DNA Electrophoresis 10% Agarose Gel
50 ml 1X TAE
30 µL ethidium bromide

DNA Electrophoresis Loading Buffer
125 mg Bromophenol blue
125 mg xylene cyanol FF
20 g sucrose

8X His-Tag Binding Buffer
2.72 g imidazole

237 g NaCl
19.36 g Tris
Adjust to 1.00 L with diH_2O
pH to 7.9

4X His-Tag Charge Buffer
52.56 g $NiSO_4$
Adjust to 500 ml with diH_2O

4X His-Tag Elution Buffer
136 g imidazole
58.44 g NaCl
4.84 g Tris
Adjust to 500 ml with diH_2O
pH to 7.9

4X His-Tag Strip Buffer
74.4 g EDTA
58.44 g NaCl
4.84 g Tris
Adjust volume to 500 ml with diH_2O
pH to 7.9

8X His-Tag Wash Buffer
5.44 g imidazole
117 g NaCl
9.68 g Tris
Adjust volume to 500 ml with diH_2O
pH to 7.9

Luria-Bertani Broth (LB)
20.0 g LB broth
1.00 L diH_2O

Luria-Bertani Agar (LB)
40.0 g LB agar
1.00 L diH_2O

MEM-Glucose
9.30 g MEM
2.20 g $NaHCO_3$
4.50 g glucose
1.00 L diH_2O
Filter sterilize

MEM-Gentamycin
9.30 g MEM
2.20 g $NaHCO_3$
50.0 ml calf serum
50.0 g gentamycin
1.00 L diH_2O
Filter sterilize

10X Phosphate Buffered Saline (PBS)
85.0 g NaCl
10.7 g sodium phosphate, dibasic
3.90 g sodium phosphate, monobasic
1.00 L diH_2O

3X SDS Sample Buffer
2.00 g SDS
10.0 ml glycerol
0.10 g bromophenol blue
5.00 ml 2- mercaptoethanol
50.0 ml diH_2O

10% SDS-PAGE Separating Gel
4.00 ml diH2O
2.50 ml 1.5 M Tris-HCl, pH 8.8
100 µl 10% SDS
3.33 ml 30% Bis:Acrylamide

12% SDS-PAGE Separating Gel
3.00 ml diH2O
2.50 ml 1.5 M Tris-HCl, pH 8.8
100 µl 10% SDS
4.00 ml 30% Bis:Acrylamide

15% SDS-PAGE Separating Gel
2.50 ml diH2O
2.50 ml 1.5 M Tris-HCl, pH 8.8
100 µl 10% SDS
5.00 ml 30% Bis:Acrylamide

5% SDS-PAGE Stacking Gel (2)
2.85 ml diH2O

1.25 ml 0.5 M Tris-HCl, pH 6.8
50.0 µl 10% SDS
1.00 ml 30% Bis:Acrylamide

SDS-Page Running Buffer
2.42 g Tris
14.41 g glycine
10.0 ml SDS
1.00 L diH_2O

50X TAE (DNA Gel Running Buffer)
242 g Tris
57.1 ml acetic acid
100 ml .5 M EDTA
Adjust to 1.00 L with diH_2O

10X Tris Buffered Saline (TBS)
12 g Tris
87.7 g NaCl
Adjust to 1.00 L with diH_2O
pH with HCl to 7.0

Tryptic Soy Broth (TSB)
25.0 g TSB broth
1.00 L diH_2O

IpaB tryptophan mutant construction

All tryptophan mutations in *ipaB* were generated using inverse PCR with pHS2-IpaB, encoding IpaB, as the template. Primers were made to encode GAGAGA, a restriction site flanking the codon to be mutated and approximately 18 nucleotides beyond the mutation site. Primers are listed in Table 2.1. Inverse PCR produced a linear fragment, which was subsequently digested with the appropriate restriction endonucleases and intramolecularly ligated. GAGAGA sequences are present at the ends of the fragment to increase the efficiency of restriction digestion. Ligation products were transformed into Nova Blue *E. coli*. Resulting plasmids were purified using the QIAGEN QIAquick™ plasmid purification kit. Purified plasmids were electroporated into the *ipaB* null *Shigella flexneri* strain SF620 and placed onto TSA plates containing Congo red and ampicillin. Ampicillin resistant, red colonies were chosen for further assays as these contained both the electroporated plasmid and the virulence plasmid based on Congo red selection. W105F was constructed to remove the natural tryptophan residue in IpaB and this was used as a template for subsequent mutants in which a Trp was introduced at novel sites.

Construction/Production of Recombinant Proteins

Mutated *ipaB* genes were subcloned from pHS2 into pACYC-Duet 1 via flanking *Nde*I and *Kpn*I sites. The resulting mutant IpaB/pACYC-Duet 1 constructs

Mutant	Primer Names	Sequence (3'-5')
W105F	B50f	GAGAGAGAGATTTAAATCCCAGCAACAGGCAAG
	B51r	GAGAGAGAGATTTAAATGCAGTAATTTTATTTGTTAATG
L133W[a]	B53f	GAGAGAGAGACGCGTGACTATGAAAAACAAATTAATAA
	B54r	GAGAGAGAGACGCGTCCATCCTTCAGTTTCAGATAGAA
F328W[a]	B57f	GAGAGAGAGGCCGCTTGGTCTGGAGGAGCCTCTCTA
	B58r	GAGAGAGAGGCGGCCGCAACAACACTAACGATAGT
I402W[a]	B59f	GAGAGAGAGGCCGGCGCTCTTGTCCTAGTT
	B60r	GAGAGAGAGGCCGGCGATTGCCCCCAGCCAAGAGCCAATCTATTTGGCTT
I574W[a]	B61f	GAGAGAGAGCTGCAGCAAACTACTGCTTGAGGC
	B62r	GAGAGAGAGCTGCAGCCATGCTTTGCAACATCAGTT

Table 2.1 Table of primers for IpaB tryptophan scanning mutants
[a]Mutations after 105 are double mutants containing W105F and the indicated mutation.

were then transformed into Nova Blue *E. coli*. Transformants were screened with Duet UP2 and T7 terminator primers. Positive plasmids were then purified using a QIAGEN QIAquick™ plasmid purification kit and then co-transformed with IpgC/pET15b into Tuner (DE3) *E. coli*. To select for bacteria containing both plasmids, transformations were plated on LB plates containing ampicillin and chloramphenicol. Each plate was resuspended in 5 ml of LB and divided evenly between 2 L of LB, each containing 100 μg/ml ampicillin and 25μg/ml chloramphenicol. Cultures were grown to mid-log phase (OD_{600} = 0.5) when protein expression was induced using 0.5 M IPTG. Induced cultures were grown for an additional three hours. Bacteria were then collected by centrifugation and resuspended in 40 ml/L of culture, with 1X His-tag binding buffer. The bacterial suspension was frozen at - 20°C.

SopE2 and Cdc42 Protein Purification

Recombinant GST-Cdc42 and GST-SopE2 were purified after being synthesized in *E. coli* BL21 (DE3). Both proteins were designed with GST fusion tags to aid in purification. Protein expression was induced by adding 0.5 M IPTG to mid-log phase bacterial cultures. After three hours, the cells were harvested by centrifugation and resuspended in 40 ml 1X PBS and then frozen at -20°C overnight. The suspension was thawed and sonicated to complete bacterial lysis and shear bacterial DNA. The insoluble material was removed by centrifugation at 12,000 x g for 12 minutes. The GST fusion proteins remained in the supernatant fraction.

Chromatography using immobilized glutathione was used to affinity purify the GST fusion proteins. For both proteins, a bed volume of 10 µl per ml of supernatant was poured for each column used. Elution was accomplished using 10 mM glutathione in 1X TBS. Proteins were dialyzed against 1X TBS to remove the glutathione from the solution. The GST protein tag was cleaved from the protein with thrombin and the released tag was removed by adsorption onto immobilized glutathione resin. The protein samples were stored at -80°C.

IpaB/IpgC and IpaC/IpgC Protein Purification

Tuner (DE3) cells containing pACYC-IpaB/pET15b-IpgC or pACYC-IpaC/pET15b-IpgC were grown in LB containing 100 µg/ml ampicillin and 25 µg/ml chloramphenicol. At mid-log phase protein expression was induced by the addition of 0.5M IPTG. Induced cultures were grown for three hours and then centrifuged at 4900 x g for eight minutes. Cell pellets were resuspended in 40 ml/L of culture with 1X His-tag binding buffer. Bacterial suspensions were frozen at -20°C.

Affinity Protein Purification of His-Tag Containing Proteins

Frozen bacterial suspensions were thawed, sonicated and clarified by centrifugation for 10 minutes at 10000 x g. Five ml of iminodiacetic acid Sepharose were washed with five column volumes (CV) of distilled water. The resin was charged with three CV of 1X His-tag charge buffer and then five CV of 1X His-tag binding buffer. Clarified supernatants were applied to the column, which was washed

with an additional five CV of binding buffer. Non-specifically bound proteins were removed with five CV of 1X His-tag wash buffer and bound proteins were then eluted in three CV of 1X His-tag elution buffer. Fractions were collected and analyzed by SDS-PAGE gel to check for protein. The resin was stripped with three CV of 1X His-tag strip buffer and stored at 4 °C.

FPLC Purification of IpaB/IpgC and IpaC/IpgC

Fractions from affinity chromotography containing IpaB/IpgC or IpaC/IpgC were pooled. EDTA and DTT were added to a final volume of 1 mM and 2 mM respectively. Samples were loaded onto a HiLoad 26/60 Superdex 200 preparative grade column equilibrated with 10 mM Tris-HCl pH 7.2, 150 mM NaCl, 0.5 mM DTT. Fractions again were analyzed by SDS-PAGE. Those fractions containing the complexes were pooled and dialyzed into sodium citrate phosphate buffer, pH 7. Proteins were stored at -80°C.

Separation of IpaB From IpgC

IpaB/IpgC was incubated at 4°C with 2% n-octyl-poly-oxyethylene (OPOE) for at least 1 hour. IpaB was separated from the chaperone using a five ml HiTrap™ Chelating HP column. The column was prepared according to manufacturer's directions. The column was washed with three CV of filtered distilled H_2O followed by 0.5 CV of filtered 1X charge buffer. An additional three CV of deionized water were applied to the column. To bind His-tagged IpgC, five CV of 1X binding buffer

with 1% OPOE was applied to the column. The IpaB/IpgC in 2% OPOE was then applied to the column and flow through fractions were collected. Sample was followed by five CV of binding buffer with 1% OPOE and then IpgC was eluted in three CV of 1X elution buffer. All fractions were checked for IpaB and IpgC through SDS-PAGE. IpaB eluted in the flow through and binding buffer fractions, while free IpgC eluted in the elution buffer.

IpaB/IpaC Complex Purification

The IpaB/IpaC pore complex was purified from an *ipaA/ipgD* null mutant *Shigella flexneri*. Bacteria were grown to OD_{600} of 1.0 in 1 L TSB with 50 µg/L of kanamycin in a shaking incubator. Bacteria were harvested by centrifugation in a swinging bucket rotor at 4900 x g for 12 minutes. Supernatants were discarded. To induce secretion of effector proteins, pellets were resuspended in ice cold 10 mM sodium phosphate, 150 mM sodium chloride and harvested a second time for 12 minutes. Bacteria were resuspended in 860 mM Congo red in 10 mM sodium phosphate, 150 mM NaCl at 37 °C. Secretion was induced by shaking the Congo red mixture at 37 °C at 200 rpm for 15 minutes. After incubation, bacteria were removed by centrifugation at 9000 x g for 20 minutes and supernatants were dialyzed against 20 mM Tris pH 7.4. Dialyzed Congo red supernatant was applied to a 5ml HiTrap™ Q sepharose FF column to remove the Congo red dye. Proteins were eluted in 20 mM Tris 1M NaCl. Fractions containing IpaB, IpaC, and IpaD were applied to a

HiLoad 26/60 Superdex 200 preparative grade column equilibrated with 1X TBS .5 mM DTT to separate the IpaB/IpaC pore from IpaD by size exclusion.

Measurement of Protein-Protein Interaction by Fluorescence Polarization

A Beacon Fluorescence Polarimeter was used to measure binding events between IpaC or SopE2 and FITC labeled Cdc42. In a 12 x 75 mm test tube FITC labeled Cdc42 was added to buffer to a concentration of 0.5 µM. 20 µM EDTA was added to chelate magnesium and finally 20 µM of GTP was added to the reaction. The reaction was then thoroughly mixed and then 5 mM magnesium was added to saturate any remaining EDTA. IpaC or SopE2 were added the reaction was allowed to incubate at 22 ºC for 30 minutes. Emission spectra were read using a Beacon Fluorescence Polarimeter. IpaC or SopE2 were added to the solution in increasing amounts and polarization was measured over time.

Gentamycin Protection Invasion Assay

Henle 407 cells were seeded on a 24 well tissue culture plate and incubated in CO_2 at 37 °C until semi-confluent. *Shigella* strains were grown at 37 °C with shaking in 10 ml of TSB to mid-log phase (OD_{600} = 0.5). One µl of the bacterial culture was added to Henle cells in MEM-glucose and centrifuged at 800 x g for five minutes to force contact. Plates were incubated for 30 minutes at 37 °C in a CO_2 incubator. Cells were then washed with MEM-gentamycin (50 grams/L) and incubated 37 °C in a CO_2 incubator for one hour in MEM-gentamycin to kill any extracellular *Shigella*.

After incubation, the MEM-gentamycin was removed by aspiration, cells were washed three times with MEM-glucose, lysed with melted agarose in deionized water and then overlaid with melted 2X LB in agar. Once the agar solidified, cells were incubated at 37°C overnight. Colonies were counted and invasion was calculated relative to complimented *Shigella* strains.

Contact Mediated Hemolysis

Shigella strains were grown to mid-log phase at 37 °C with shaking in 10 ml of TSB. Bacteria were collected by centrifugation at 3200 x g. Bacteria were resuspended in 200 µl of 1X PBS. Sheep erythrocytes were washed at room temperature with 1X PBS and resuspended in 1X PBS to the original cell concentration. Fifty µl of red blood cells (RBCs) were aliquoted into a 96 well microtiter plate to which 50 µl of the bacterial cell suspension was added per well. Contact was induced by centrifugation at 2500 x g at 22 °C for 10 minutes. Microtiter plates were then incubated at 37°C for 1 hour. After incubation, RBC/bacterial pellets were vigorously resuspended in ice cold 1X PBS and centrifuged at 2500 x g for 15 minutes at 4°C. Supernatants were transferred to clean empty wells. Hemoglobin release was measured by monitoring absorbance at 545 nm on a µQuant™ microtiter plate reader.

TCA Precipitation of Secreted Proteins

Shigella strains were grown in 10 ml of TSB overnight in a shaking incubator at 37°C. Overnight cultures were centrifuged at 4000 rpm for 10 minutes at 4°C.

Supernatants were transferred to glass Corex tubes. Pellets were resuspended in 200 µl of deionized water, 150 µl 3X sample buffer and 10 µl 1.5 M DTT. Pellets were then frozen at -20°C for future use. 1.1 ml of ice cold 100% trichloroacetic acid (TCA) was added to supernatants and after 30 minutes, the sample centrifuged at 9000 x g for 12 minutes. Supernatants were discarded and remaining pellets were washed with 10 ml of ice cold 5% TCA and centrifuged. Supernatants were discarded and pellets were washed twice in 10 ml of ice cold acetone. After the acetone washes, Corex tubes were inverted to dry pellets. Final samples were resuspended in 400 µl of cold 1X PBS, 200 µl 3X sample buffer and 15 µl 1.5 M DTT. Samples were then seperated on a 15% resolving SDS-PAGE gel.

Western blot

To analyze the presence of proteins in bacteria and supernatant samples from trichloroacetic acid precipitations were run on a 15% resolving SDS-PAGE gels and the gels were incubated in 1X blotting buffer for 20 minutes. Seperated proteins were blotted onto nitrocellulose using a BioRad Transblot-SD Semidry Transfer Cell for 35 minutes at 15V at constant voltage. After blotting, the nitrocellulose membrane was incubated in 1X blocking buffer for 45 minutes and in primary antibody diluted 1:1000 at 4 °C overnight. Nitrocellulose membranes were washed in 1X PBS-Tween 20 three times for five minutes each. Membranes were incubated with secondary antibody diluted 1:10,000 for 1 hour at room temperature. Membranes were then washed an additional three times with 1X PBS-Tween 20 and finally, twice with 1X

PBS for five minutes with shaking. Membranes were then scanned on a Li-Cor Odyssey™ Infrared scanner and imaged using the Odyssey Software.

Circular Dichroism Spectroscopy of Purified Proteins and Protein Complexes

Far UV CD spectra and thermal unfolding monitoring at 222 nm were performed using a Jasco J720 spectropolarimeter. Far UV spectra were collected at a wavelength range of 190 to 260 nm at a scan rate of 20 nm/min. A 0.1 cm path length cell quartz cuvette was employed and spectra were acquired in triplicate and averaged. The thermal-induced unfolding transitions were acquired using a 0.1 cm path length cell quartz cuvette with a temperature ramping rate of 15°C per hour. Protein concentrations ranged from 1 to 10 μM with all experiments performed in phosphate citrate buffer (pH 7) to minimize pH shifts induced by temperature. CD signals were converted to molar ellipticities to normalize for differences in protein concentration and the unfolding transitions were analyzed using the Jasco Spectral Manager™ and Sigma Plot softwares.

Preparation of Phospholipid Vesicles

Aliquots of DOPC, DOPG, and cholesterol in chloroform were dried under helium and vacuum for 3 hours to create lipid films. DOPC:DOPG (w/w) and DOPC:DOPG:cholesterol (w/w/w) concentrations varied based on desired lipid composition. Lipid films were rehydrated in 100 mM sulforhodamine B (SRB) in water by incubating at room temperature for 10 minutes and then resuspended by

using a pipette. Rehydrated films were sonicated for 15 seconds and extruded through a 100-nm pore size membrane 10 times at 45^{o}C. To remove untrapped dye, extruded SRB containing liposomes were loaded onto a Sephadex G-50 gel filtration column equilibrated with 1X PBS or 1X TBS. Peak fractions were selected visually. Fractions were stored at 4^{o}C and used within one week.

Monitoring Rhodamine Release From Phospholipid Vesicles

SRB release from phospholipid vesicles was monitored using a SPEX FluoroMax™ spectrofluorometer. Baseline fluorescence was measured for 30 seconds. Protein was added and SRB release was detected as an increase in fluorescence intensity over time for 250 seconds. Triton X-100 (0.1%) was added to completely disrupt liposomes as a control for complete SRB release. IpaD was used as a negative control for liposome disruption.

CHAPTER 3

Potential IpaC protein interactions with IpgC

Introduction

Bacterial Secretion Systems

Many gram negative pathogens utilize secretion systems to deliver virulence factors to targeted host cells. To date, six distinct bacterial secretion systems have been identified in bacteria. Type II and type V secretion systems are Sec-dependent, requiring the general secretory pathway (Sec components) for protein translocation across the inner membrane. The Sec pathway catalyzes and translocates proteins across the bacterial inner membrane to the periplasmic space. Type I, type III, type IV secretion systems are Sec-independent (Harper and Silhavy, 2001). A sixth secretion system has recently been described in *Vibrio cholerae, Pseudomonas aeruginosa*, and *Burkholderia cneocepaciae*, but to date, very little is known about this system.

Type I secretion systems contain an ATP-binding cassette (ABC), a membrane fusion protein and an outer membrane component. Type I secretion allows secretion across the inner and outer membranes in a single step (Fath and Kolter, 1993). Type II secretion pathways are composed of 12-14 protein components that interact with the Sec-pathway. Proteins targeted for transport through the type II secretion system are exported from the cytoplasm to the periplasm via Sec-machinery. The type II secretion system then transports the protein from the

periplasm to the extracellular environment (Russel, 1998). Type III secretion systems are composed of 25 or more protein components and allow direct, ATPase driven transport of virulence factors from the bacterial cytoplasm to the cytoplasm of targeted host eukaryotic cells. Protein transport in type III secretion is Sec-independent and is also referred to as contact dependent secretion (Hueck, 1998). Type IV secretion systems were first identified as conjugal transfer systems that transferred bacterial DNA into targeted bacterial hosts. These pilus-like transport systems have now been implicated in exporting multisubunit and monomeric proteins (sometimes directly into eukaryotic target cells) in addition to DNA (Winans, *et al.*, 1996). Type V secretion systems are autotransporter systems that work in conjunction with Sec proteins. Proteins exported by the type V secretion system are large multidomain proteins consisting of five regions; a Sec-dependent signal domain, the mature portion of the protein, and the α-, β- and γ-regions. The Sec machinery uses the Sec signal to move the protein from the cytoplasm to the periplasm. The β-region then inserts and forms a pore in the outer membrane. The remaining regions of the protein pass through this pore, are cleaved by autoproteolysis and released to the extracellular environment. They are further processed through subsequent autoproteolysis events (Klauser *et al.*, 1993). Type VI secretion systems have been identified in several gram negative organisms, but the structure and mechanism of this secretion system has yet to be characterized (Aubert *et al.,* 2008) (Zheng and Leung, 2007) (Pukatzki *et al.,* 2006).

S. flexneri utilize type III secretion to promote pathogen uptake in targeted epithelial cells of the large intestine (Sansonetti *et al.*, 1982). Upon host cell contact or conditions that mimic host cell contact, the *S. flexneri* type III secretion system (TTSS) exports effector proteins through the external needle apparatus and to the membrane and cytoplasm of targeted host cells. "Early" effector proteins, IpaB and IpaC, bind to one another following their export and form the "translocon" within the host cell membrane. The IpaB/IpaC translocon inserts into host cell membranes and forms a pore through which subsequent effector proteins can pass into the targeted host cell's cytoplasm for promoting bacterial invasion (Davis *et al.,* 1998) (Blocker *et al.,* 1999). In the absence of the translocon, entry into targeted cells cannot proceed (Menard *et al.,* 1993). Prior to receiving the signal for secretion, IpaB and IpaC are partitioned to the bacterial cytoplasm where they bind independently to IpgC, waiting in queue until they are secreted by the type III secretion apparatus (TTSA) (Menard *et al.,* 1994, Page *et al.,* 1999).

The Molecular Chaperone IpgC

Invasion plasmid gene C (IpgC) is the molecular chaperone for the translocator proteins IpaB and IpaC in *S. flexneri*. Chaperones of type III secretion systems fall into three classes. Class I chaperones are those associated with late effector proteins. Class I can be further divided into class IA and IB based on their association with one or multiple effector proteins, respectively. Class II chaperones bind to known or proposed translocator proteins, while class III chaperones are

associated with proteins within the flagellar system (Cornelis and Gijsegem, 2000, Page *et al.,* 2001).

IpgC is a class II chaperone of the *S. flexneri* type III secretion system (Page *et al.*, 2001). Like all other chaperones from type III secretion systems, IpgC is small (17 kDa), possesses a highly acidic pI (4.6) and serves multiple roles as a part of the TTSS. As previously mentioned IpgC binds separately to IpaB and IpaC. These associations serve several purposes. As mentioned in the introduction, one function is to prevent IpaB and IpaC from associating with each other while still in the bacterial cytoplasm. This prevents aggregation of the early effector/translocator proteins within the bacterial cytoplasm and premature formation of the translocon pore (Menard *et al.*, 1994a). Additionally, IpgC has been proposed to hold both IpaB and IpaC in a secretion competent state. Due to the large sizes of the translocator proteins, it is evident that secretion of each IpaB and IpaC would have to occur with the protein in some form of elongated state in order to accommodate the small inner diameter (~2.5 nm) of the needle apparatus (Blocker *et al.,* 1999). It has been shown here and elsewhere that in the absence of IpgC, IpaB and IpaC can insert into and disrupt liposomes (DeGeyter *et al.,* 1997). However, when IpgC is bound to the effector proteins, this liposome destabilizing activity is blocked (Birket *et al.,* 2007). When IpgC is absent in the bacterium, IpaB and IpaC are thus degraded to similarly protect the bacterial cytoplasmic membrane (Menard *et al.,* 1994).

In addition to its chaperone function, IpgC has been shown to serve as a transcriptional co-activator of *virA* and *ipaH*9.8 (Munson *et al.,* 2008). It has been

demonstrated that IpgC can be co-purified with MxiE, suggesting that it works in conjunction with MxiE to increase both the expression of VirA and IpaH9.8 (Munson *et al.,* 2008). Initially, this association was thought to be transient but it is now proposed to only be possible upon release of IpaB and IpaC from IpgC, indicating the increase in transcription of the above proteins is signaled only after the translocon has been formed and IpgC released from its translocator protein partner (Munson *et al.,* 2008).

Because IpaC and IpaB possess little or no sequence homology with each other, the manner and ability of IpgC to bind both proteins is of great interest. IpaC is a 42-kDa protein consisting of several key functional and structural regions (Figure 3.1). Within these regions are a transmembrane domain, a putative coiled-coil region and a TTSS secretion signal. IpaC has multiple functions as a *Shigella* virulence determinant. It has been demonstrated to disrupt liposomes, promote invasion of epithelial cells, and interact with actin and small signaling molecules (Picking *et al.*, 2001) (Kueltzo *et al.*, 2003). Additionally, the 19 C-terminal amino acids of IpaC are proposed to make up a distinct effector region of the protein. Here we investigate the influence of IpgC binding on IpaC structure and function and the importance of IpaC's C-terminal tail in IpaC invasion function (Picking *et al.*, 2001)

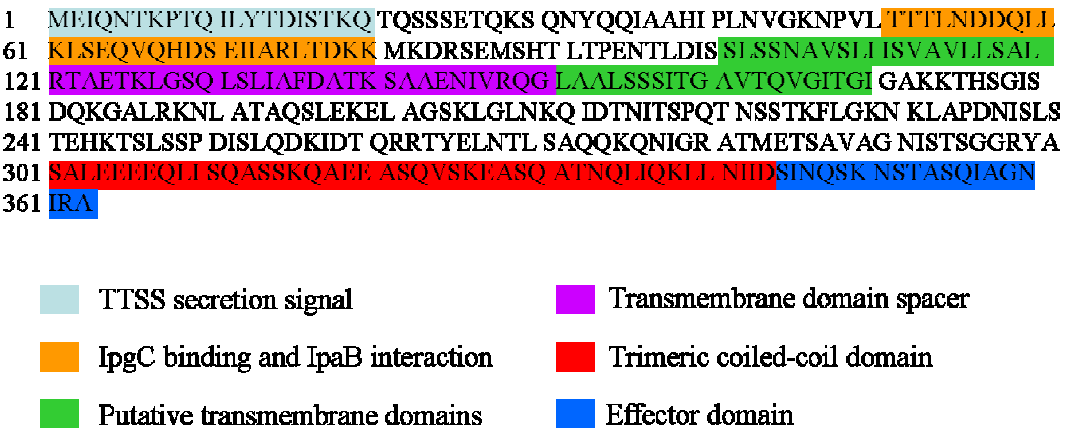

Figure 3.1 Schematic diagram of regions of IpaC. Residues 1-20 encode a TTSS. Residues 50-80 are required for binding and interactions with IpgC and IpaB. Amino acids 100-120 and 150-170 are transmembrane domains while 120-150 form a loop between to the two transmembrane domains. Residues 300-344 are a putative trimeric coiled-coil and the penultimate 19 amino acids of IpaC are involved in effector function.

Results

IpaC/IpgC Protein Purification

Purification of IpaC/IpgC complexes is achieved through co-expression of both IpaC and His-tagged IpgC in Tuner (DE3) *E. coli*. This association inside *S. flexneri* maintains IpaB and IpaC as part of a soluble complex, prevents IpaB association with IpaC and prevents IpaC from being targeted for degradation in the bacterial cytoplasm as part of a premature translocon complex (Birket *et al.*, 2007). Large quantities of recombinant IpaC/IpgC complex can be prepared by affinity chromatography. After initial complexes made in *E. coli* are prepared by Ni^{+} affinity chromatography, they can then be separated from free IpgC by size exclusion chromatography (Figure 3.2). It has been demonstrated that the effector/chaperone complex PopD/PcrH, of the type III secretion system of *P. aeruginosa,* can be separated into its component proteins by decreasing the pH of the buffer. Because of similarities between the *S. flexneri* IpaC/IpgC complex and the *P. aeruginosa* effector/chaperone complex, the same method of decreasing the protein's environmental pH to release the chaperone was employed (Schoehn *et al.*, 2003). Upon lowering the pH to 5.0 the translocator/chaperone complex was partially separated into its component proteins and these were further separated by a second size exclusion chromatography step (Figure 3.2). This provides a convenient method for purifying IpaC in the absence of chaotropic agents such as urea, which has always been a difficulty in the study of this protein.

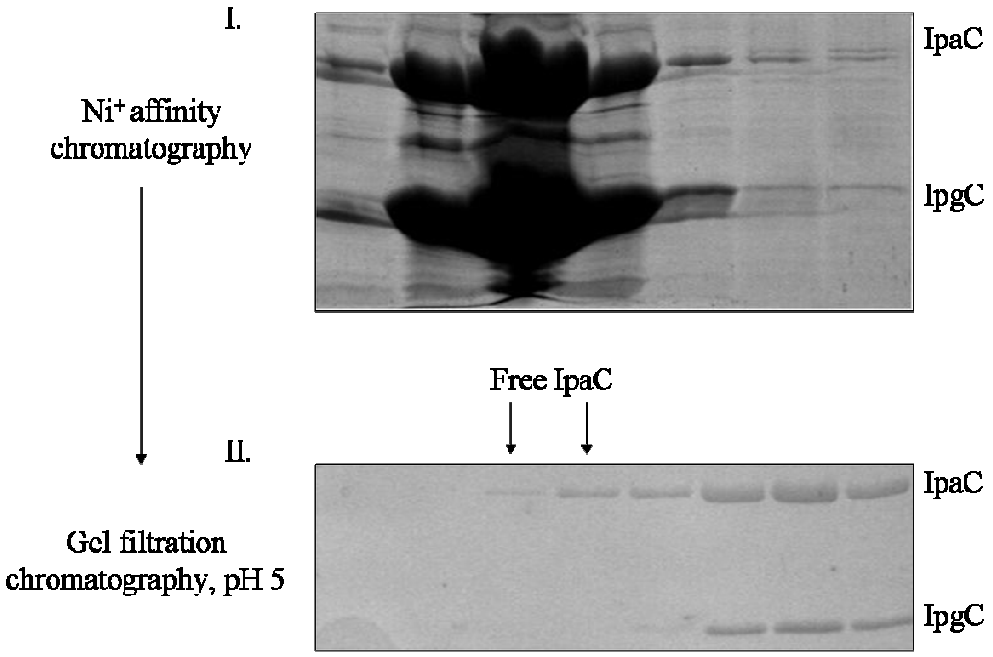

Figure 3.2 Purification of IpaC/IpgC complex and purified IpaC.
I. IpaC/IpgC complexes were coexpressed in *E. coli* and were purified by affinity chromatography. Peak fractions were determined by SDS-PAGE.
II. IpaC was separated from IpgC by lowering the solution pH to 5 and purified by Superdex 16/60 size exclusion column chromatography. IpaC freed from the IpaC/IpgC complex is labeled. Free IpgC elutes later at a lower molecular weight (not shown). Peak fractions were analyzed using SDS-PAGE.

Circular Dichrosim Spectroscopy of the IpaC/IpgC complex

Circular dichroism (CD) spectroscopy is a useful tool for determining changes in the global secondary structure of proteins. CD spectroscopy uses circularly polarized light to measure the differences in the adsorption between left and right handed polarized light. Because chiral molecules, such as the α-carbon of the peptide backbone, exhibit measurable differences in CD, we can use these measurements to provide an estimate of the global secondary structure content of proteins within a sample. Secondary structure components produce characteristic UV spectra with characteristic peaks and valleys at specific wavelengths (Bloemendal and Jiskoot, 2005). Far UV spectra of IpaC, IpgC and IpaC/IpgC complexes as monitored by CD reveal that IpgC does significantly influence IpaC structure (Figure 3.3). In order to quantify secondary changes far UV spectra were analyzed using the freeware Dichroweb. Dichroweb uses a wide range of databases to compare experimental data to known protein structures and spectra (Lobley *et al.*, 2002). Dichroweb analysis confirms that upon IpgC binding α-helical structure of IpaC increases from 30% to 53%, while the β-sheet content decreases significantly from 22% to 8% (Table 3.1). This suggests that upon IpgC binding IpaC undergoes a significant conformational change, resulting in a loss of β-structure compensated by an increase in α-helicity (Birket *et al.,* 2007).

Thermal unfolding as monitored by CD supports these findings. Thermal unfolding or melting temperatures of proteins can be determined by monitoring α-helical proteins at 222 nm over increasing temperatures. As the temperature

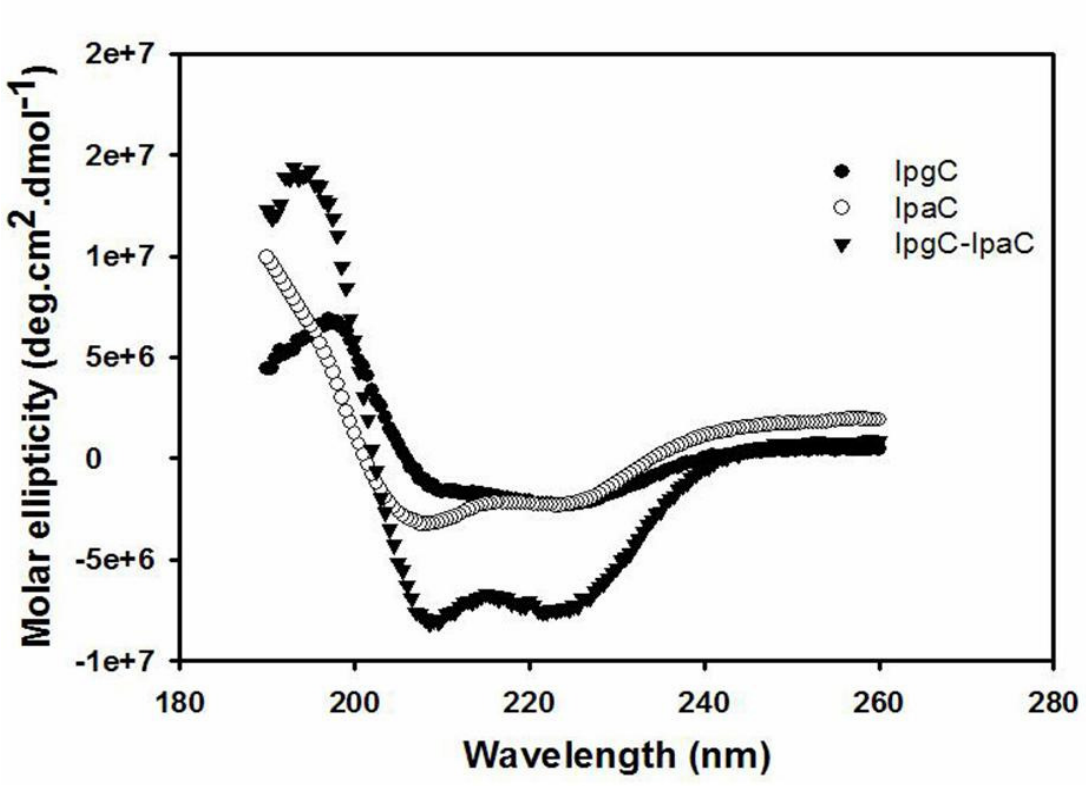

Figure 3.3 Far UV CD spectra and thermal melting temperatures of purified IpaC, IpgC and IpaC/IpgC complexes.
Far UV spectra of purified proteins and protein complexes using circular dichroism was measured at a wavelength range of 190 to 280 nm. Spectra are an average of at least two representative spectra. (Birket et al. 2007)

Protein	α-helix	β-sheet	Turns	Random
IpaC	0.30	0.23	0.18	0.31
IpgC	0.52	0.21	0.11	0.17
IpaC/IpgC[a]	0.42	0.22	0.14	0.24
IpaC/IpgC[b]	0.53	0.08	0.12	0.28

Table 3.1 Deconvolution of the far-UV CD spectra for purified IpaC, IpgC and IpaC/IpgC complexes.
Deconvolution of the far-UV spectra as analyzed by Dichroweb using SELCOM and CONTIN algorithms. [a] Calculated or theoretical sums of secondary structure elements. [b] Experimentally derived values for the binary complex as determined by far-UV CD spectroscopy (Birket *et al.,* 2007).

Protein	Melting Temperature (T_m) ± SE, °C
IpaC	45.5 ± 0.3
IpgC	53.9 ± 0.2
IpaC/IpgC	56.3 ± 0.1

Table 3.2 Thermal melting temperatures of purified IpaC, IpgC and IpaC/IpgC complexes.
Thermal melting temperatures were monitored at 222 nm to probe changes in α-helical content over increasing temperature (Birket *et al.,* 2007).

increases, proteins depart from their normal structured state to assume a state that is much more disordered (Bloemendal and Jiskoot, 2005). This transition can be fitted to a sigmoidal curve and the midpoint of this curve can be used to determine the thermal melting or unfolding temperature of the protein in the sample. Monitoring the thermal transitions of purified IpaC, IpgC and IpaC/IpgC complexes reveal that upon complex formation the thermal melting temperature of IpaC and IpgC are significantly increased from 45.5 °C to 56.3 °C and 53.9 °C to 56.3 °C (Table 3.2). These data further support that chaperone binding strongly influences and increases IpaC protein structure and stability.

Scanning Mutagenesis of the IpaC C-terminal Tail

Previous structure function analyses have revealed key regions within IpaC important in secretion, IpgC and IpaB binding, cell signaling and invasion (Picking *et al.,* 2001) (Harrington *et al.,* 2003). More specifically, the 19 most C-terminal amino acids of IpaC have been determined to play an important role in invasion and actin nucleation (W.D. Picking, unpublished results). In order to fully characterize this region, scanning mutagenesis was performed to identify specific residues important in IpaC effector function. Deletion of this region abolishes the ability of the bacterium to invade Henle 407 cells, but does not significantly impact its ability lyse sheep erythrocytes (W.L. Picking, B.M. Hoffman, K. Flentie, unpublished data). The ability of *S. flexneri* to lyse red blood cells (contact hemolysis), is indicative of IpaBC pore formation and insertion into the plasma membrane of red blood cells

(RBC's) (Clerc *et al.,* 1987) (Hakansson *et al.,* 1996) (Blocker *et al.,* 1996). Scanning mutagenesis of this region reveals several residues important for *S. flexneri* invasion within this region, including S345, I346, N347, A354 and I357. Substitutions at these amino acids result in a significant loss in invasion (Table 3.3). The 19 most C-terminal residues of IpaC and the *Salmonella* homologue, SipC, are relatively well conserved between the two proteins, differing only at five residues (Kaniga *et al.*, 1995). Additionally, it has been demonstrated that SipC's actin nucleation function lies within the C-terminal half of the protein, which has recently been shown to be true for IpaC (Hayward and Koronakis, 1999) (Kueltzo *et al.*, 2003). In order to determine the importance of these unconserved residues in IpaC, mutations were made individually to four of the five unconserved residues in IpaC (N351A, T353A, A354L, Q356A). While three of the four mutations did not exhibit a significant decrease in invasion individually, alanine substitution at 354 did exhibit a 29% decrease in invasion. To mirror the SipC tail even more closely, double and triple substitutions were made at residues 351, 353 and 356. These mutations also resulted in a significant reduction in the invasion phenotype (Table 3.3), suggesting that while these residues do not appear to act significantly on an individual basis, they may act as a group to facilitate invasion.

To ensure that these proteins were still being expressed and not degraded by *S. flexneri*, western blot analysis was performed. Those mutants exhibiting levels of invasion 75% or lower than wild type were grown overnight and resulting pellets

Mutant Name	345 365	Relative Invasion (± SE)[a]
IpaC (wt)	SINQSKNSTASQIAGNIRA	100 ± 12
79	**A**INQSKNSTASQIAGNIRA	23 ± 14
78	S**S**NQSKNSTASQIAGNIRA	9 ± 7
77	SI**L**QSKNSTASQIAGNIRA	73 ± 8
76	SIN**L**SKNSTASQIAGNIRA	102 ± 5
75	SINQ**A**KNSTASQIAGNIRA	100 ± 9
74	SINQS**I**NSTASQIAGNIRA	95 ± 4
73	SINQSK**A**STASQIAGNIRA	95 ± 6
72	SINQSKN**A**TASQIAGNIRA	93 ± 3
71	SINQSKNS**A**ASQIAGNIRA	93 ± 15
70	SINQSKNST**L**SQIAGNIRA	71 ± 25
61	SINQSKNSTAS**A**IAGNIRA	101 ± 2
62	SINQSKNSTASQ**S**AGNIRA	32 ± 15
63	SINQSKNSTASQI**S**GNIRA	82 ± 38
64	SINQSKNSTASQIA**S**NIRA	100 ± 10
82	SINQSKNSTASQIAG**Q**IRA	90 ± 36
83	SINQSKNSTASQIAG**A**IRA	99 ± 5
65	SINQSKNSTASQIAGN**S**RA	97 ± 8
66	SINQSKNSTASQIAGNIR**I**	99 ± 10
7161	SINQSKNS**A**AS**A**IAGNIRA	58 ± 31
9361	SINQSK**A**S**A**AS**A**IAGNIRA	29 ± 19

Table 3.3 The effect of scanning mutagenesis on the IpaC C-terminal tail
Scanning mutagenesis of the 19 amino acid effector region of IpaC. All mutants in the table above have a relative hemolysis of 100% compared to IpaC wild-type (wt).
[a] Relative invasion is determined as a percentage to IpaC wild type (W.L. Picking, B.M. Hoffman, K. Flentie, unpublished data).

were probed for IpaC using anti-rabbit IpaC antibodies (R66). All IpaC proteins were expressed at levels comparable to wild type *S. flexneri* (Figure 3.4).

IpaC Does Not Appear to Directly Interact with Cdc42

It is widely accepted that the small Rho GTPase Cdc42, plays a role in *Shigella* invasion. It was thus proposed that IpaC may directly interact with Cdc42 to induce invasion (Adam *et al.*, 1995, 1996) (Tran Van Nhieu *et al.*, 1999). In *Salmonella typhimurium*, the IpaC homologue SipC is essential for invasion. However, it is the guanine exchange factor (GEF) SopE2, not SipC, that has been demonstrated to interact directly with Cdc42 and direct actin polymerization (Bakshi *et al.*, 2000) (Stender *et al.*, 2000). Interestingly, SopE2 shares absolutely no sequence homology with IpaC and there is no known homologue of SopE2 in *Shigella*. In order to investigate the relationship between IpaC and Cdc42, fluorescence polarization (FP) was utilized to assess the ability of these two proteins to interact directly.

Fluorescence polarization is a form of fluorescence spectroscopy that provides a sensitive measure of rotational diffusion of molecules in solution. In solution, molecules move at a rate inversely related to their molecular volume. Larger molecules thus rotate more slowly in solution, while smaller molecules rotate faster (Lakowicz, 1983). Due to the sensitivity of FP, changes in the rotational diffusion rate of a fluorescently tagged molecule, upon binding to a nonfluorescent molecule can be accurately measured as an increase in FP value. If a molecule is capable of

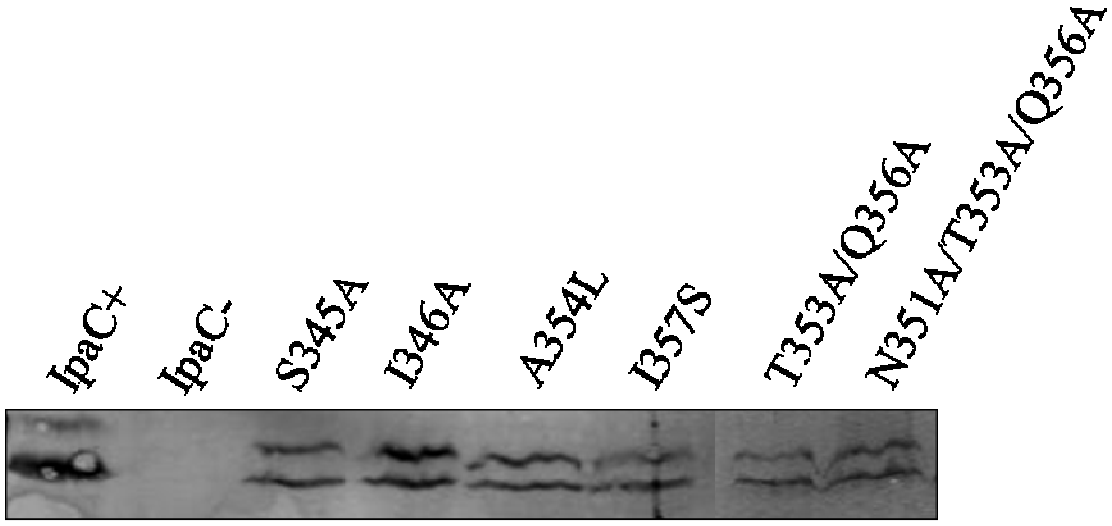

Figure 3.4 Western blot analysis of IpaC C-terminus mutants demonstrating poor invasive phenotypes

To ensure that all IpaC C-terminal mutants were expressing *ipaC*, Western blots were performed on pellets of the IpaC C-terminal mutants demonstrating a relative hemolysis of 75% or lower. IpaB and IpaC mutants at times appear as doublet bands upon Western blot analysis.

binding to the fluorescently tagged molecule in solution, thereby creating a larger complex, the polarization value increases (Lakowicz, 1983). Using fluorescently labeled Cdc42, FP was used to determine the ability of Cdc42 to bind IpaC. Increasing amounts of IpaC were titrated with FITC-labeled Cdc42 and the change in polarization was measured. SopE2 binding of FITC-Cdc42 was used as a positive control. Although, SopE2 caused a significant increase in the polarization value (mP) of FITC-Cdc42, IpaC did not induce a change in the polarization value of FITC-Cdc42 (Figure 3.5). Nanomolar concentrations of SopE2 were enough to cause increases in FITC-Cdc42 polarization while, in contrast high concentrations of IpaC where unable to induce any change in FITC-Cdc42 polarization. Nearly identical results were obtained when the assay was carried out with FITC-Cdc42 pre-incubated with GTP (data not shown). These data suggest that IpaC does not directly associate with Cdc42.

Discussion

Within the *S. flexneri* type III secretion system, IpaC has been shown to serve multiple functions. It possesses the ability to disrupt liposomes, promote invasion of epithelial cells, bind to its translocator protein partner IpaB and bind to its chaperone IpgC (Picking *et al.*, 2001) (Kueltzo *et al.*, 2003). IpgC association with IpaC prevents protein degradation and aggregation within the bacterial cytoplasm and has also been proposed to hold IpaC in a secretion competent state (Blocker *et al.*, 1999). To date, few data have been obtained describing this association.

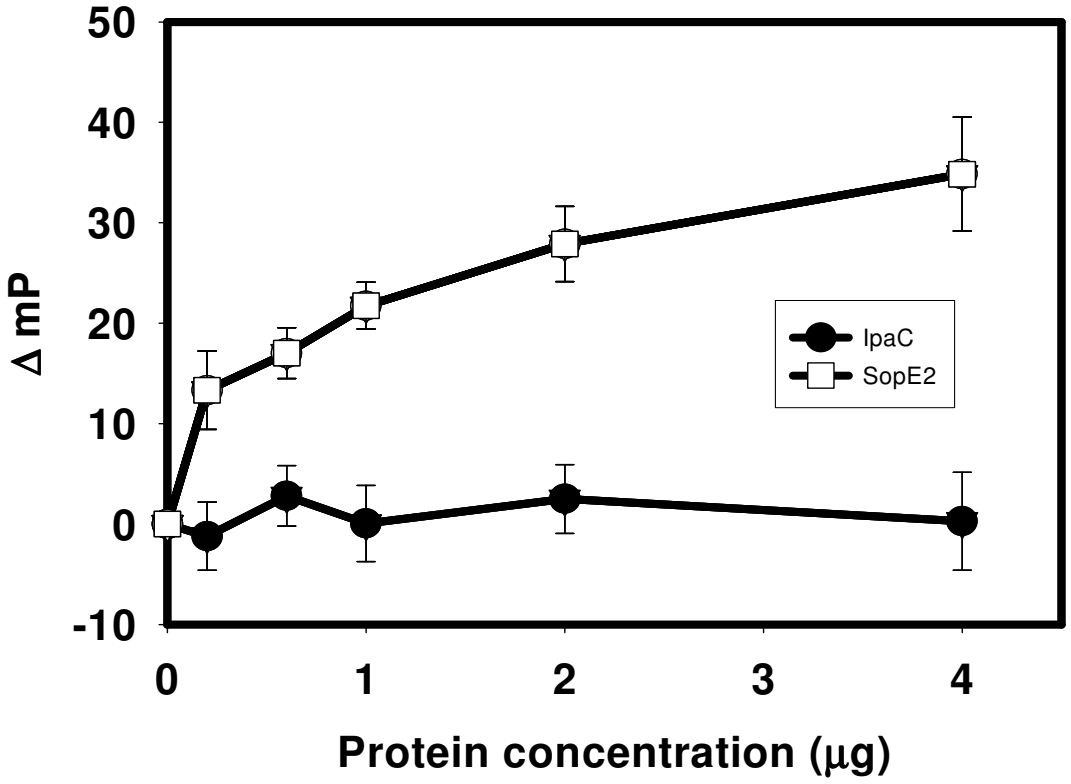

Figure 3.5 Effect of IpaC binding on the emission of FITC-labeled Cdc42.
The effect of IpaC and SopE2 on FITC-labeled Cdc42 was determined using 0.5 μM of FITC-Cdc42 and increasing concentrations of IpaC and SopE2. The data shown are representative of at least three assays and were obtained with GTP bound to FITC-Cdc42.

Here we have demonstrated that the IpaC/IpgC complex can be purified from an *E. coli* expression system in a highly soluble and stable state. Circular dichroism spectroscopy data show that upon IpgC binding, the IpaC α-helical content increases significantly, while its β-sheet composition decreases. Additionally, thermal melting experiments show an increase in protein melting temperature. These data suggest that IpgC association not only significantly induces conformational changes in IpaC but it also stabilizes the protein's overall structure. The inner diameter of the needle of the *S. flexneri* TTSA measures approximately 2.5 nm (Blocker *et al.*, 2001) and IpaC possesses a relatively large molecular mass (42 kDa). It would thus be unlikely that IpaC could be secreted through the needle in its fully folded state. To accommodate these size restraints, it has been predicted that IpaC must pass through the needle in an alternative conformation. Changes in protein conformation, as detected by circular dichroism, support the proposal that IpgC holds IpaC in a secretion competent state prior to passage through the needle apparatus.

In addition to addressing the influence of IpgC binding on IpaC, we also investigated the effector function of IpaC. Deeper investigation into the C-terminus of IpaC demonstrated that not only are the 19 most C-terminal amino acids of IpaC required for *S. flexneri* invasion, but specific amino acids appear to play a vital role in invasion-related communication with the host cell. Point mutations at positions 345, 346, 347, 354 and 357 significantly lower levels of invasion. Additionally, in attempts to make IpaC more like its *Salmonella* homologue, double and triple mutations at residues 351, 353 and 357 resulted in a dramatic decrease in

invasiveness. These results indicate that the 19 amino acid C-terminal tail region plays a vital role in bacteria-host cell communication. We do not yet know how these mutations influence the structure of this portion of IpaC.

As previously described, *S. flexneri* utilizes type III secretion to induce membrane ruffling and cytoskeletal rearrangements within the host cell. This eventually results in entry of the pathogen in a process that visually resembles phagocytosis. In order to facilitate this, effector proteins of the TTSS must utilize cell signaling pathways to direct cytoskeleton and membrane components. It has been shown that small Rho GTPases play a significant role in this process, especially Cdc42. Thus, it has been proposed that IpaC interacts directly with Cdc42, though how this interaction occurs has yet to be demonstrated (Adam *et al.*, 1995, 1996) (Tran Van Nhieu *et al.*, 1999). Fluorescence polarization data in this Chapter shows that IpaC is unable to bind to FITC-labeled Cdc42. This data demonstrates that IpaC does not directly interact with Cdc42 and IpaC's role in mediating host cytoskeletal rearrangements is through a different set of interactions that alter host cell signaling.

CHAPTER 4

Analysis of the IpaBC pore complex

Introduction

A number of gram-negative pathogens utilize type III secretion systems to move effector proteins from the bacterial cytoplasm into the cytoplasm of a host cell. Although, the TTSS is a large apparatus composed of 25 or more proteins at various copy numbers, many of the proteins are conserved among bacterial genera, particularly those associated with the apparatus structure. Some proteins are conserved at the sequence level while others are conserved structurally or functionally. One such conserved structural component in this class of secretion systems is the translocon. Initially, the term translocon was coined to describe sites within the endoplasmic reticulum at which protein co-translational translocation occurred into the rough endoplasmic reticulum lumen, but today the term has broadened to include a number of diverse protein-translocation systems (Schnell and Herbert, 2003). In type III secretion, the translocon is a multiprotein transmembrane complex that spans the plasma membrane of the target cell and connects it with the type III secretion apparatus of the bacterium. This protein complex is proposed to form a channel through which the type III secretion apparatus is able to inject proteins directly into the host cell cytosol (Buttner and Bonas, 2002).

In bacterial type III secretion, host cell contact induces secretion of effector proteins through the needle apparatus to the targeted eukaryotic cell (Harper and

Silhavy, 2002). The first proteins secreted actually insert into the host cell plasma membrane to form the pore translocon pore (Blocker *et al.,* 1999). The translocon proteins may have host-altering effector functions of their own, but this is not necessarily a universal trait of this class of proteins. The major role of the pore translocation complex is to permit later effectors access to the host cell cytoplasm via the TTSS (Blocker *et al.,* 1999). Because translocon formation is a conserved theme throughout type III secretion, pore complexes have been found and are well-studied in a number of Gram-negative pathogens including YopBD in *Yersinia* spp., PopBD in *P. aeruginosa*, EspBD in *E. coli,* and IpaBC in *S. flexneri* (Hakansson *et al.,* 1993) (Menard *et al.,* 1994b) (Kenny *et al.,* 1996) (Hauser *et al.,* 1998).

The IpaBC tranlocon complex

Like most other known translocator proteins, IpaB and IpaC both contain putative transmembrane regions and are known to associate with membranes *in vitro* (Menard *et al.,* 1994a) (DeGeyter *et al.,* 1997) (DeGeyter *et al.,* 2000). In the absence of the translocator proteins, late effector proteins are not secreted into the host cell, though they can be secreted into the bacterial culture supernatant (Menard *et al.,* 1994b). Each translocon component protein has distinct structural and functional characteristics. As mentioned in the Introduction, IpaB has been implicated in controlling type III secretion of effector proteins as well as having an effector function associated with macrophage apoptosis (Menard *et al.,* 1994b) (Zychlinsky *et al.,* 1994). In contrast, IpaC does not appear to possess regulatory function with

regard to type III secretion and is not required for inducing macrophage apoptosis; however, IpaC does play an important role as an effector function by promoting invasion after directly influencing actin nucleation within targeted cells (Menard *et al.,* 1996) (Tran Van Nhieu *et al.,* 1999) (Kueltzo *et al.*, 2003). How these proteins work together is still poorly understood.

The investigation of translocator component proteins has been done largely on IpaB and IpaC as individual proteins. Although it is generally accepted that the IpaBC complex forms a pore in eukaryotic cells, the complex itself has yet to be characterized (Menard *et al.,* 1994b) (Blocker *et al.,* 1999). Here, we show that the IpaBC translocon complex can be purified as a soluble complex from *S. flexneri.* Purified complexes were then used to further characterize IpaBC's interactions with artificial phospholipid liposomes and to begin studies on the structural aspects of the translocon complex. This information should be useful in understanding the physical nature of translocon complexes from other gram negative bacterial pathogens.

Results

Purification of the IpaBC pore complex

It was discovered by Parsot *et al.,* that in the absence of a target host cell, secretion of the type III effector proteins from *Shigella flexneri* could be induced by the addition of the small amphipathic dye Congo red to growing cultures at 37 °C (Parsot *et al,* 1995). After Congo red induction, culture supernatants contain high quantities of the effectors IpaA, IpaB, IpaC, IpaD and IpgD. It has also been determined that other

dyes similar in structure to Congo red, including Evan's blue and brilliant orange, are able to induce similar levels of secretion by the *Shigella* type III secretion machinery (Bahrani *et al.,* 1997). All three molecules are amphipathic and symmetrical comprised of two amino-substituted naphthalenesulfonate groups connected by azo linkages to a central biphenyl group. How this molecule interacts with the TTSA is unknown.

Using Congo red induction, the IpaBC translocon can accumulate at significant concentrations in bacterial supernatants and purified as a soluble complex from *S. flexneri*. Because the effector proteins IpaA and IpgD co-purify with but do not associate with the IpaBC pore complex, the translocon is expressed from an *ipaA/ipgD* null *Shigella flexneri* strain (personal observation). The absence of IpaA and IpgD reduces the virulence of the organism somewhat, but the pathogen retains its ability to invade cultured cells and to carry out contact mediated hemolysis. Using this strain also permits safer handling of large volume of cultures. Following Congo red induction of *ipaA/ipgD S. flexneri,* IpaB IpaC and IpaD are secreted extracellularly. The Congo red supernatant is then loaded onto an anion exchange Q-Sepharose column. The differently charged proteins (IpaB, IpaC and IpaD) can then be separated from the amphipathic Congo red dye by their elution in 1M NaCl. Once the Congo red has been removed from the sample, IpaD can be separated from the IpaBC pore complex using gel filtration chromatography (Figure 4.1).

By comparing the IpaBC complex to gel filtration retention times of known proteins the apparent molecular weight of the IpaBC complex can be estimated

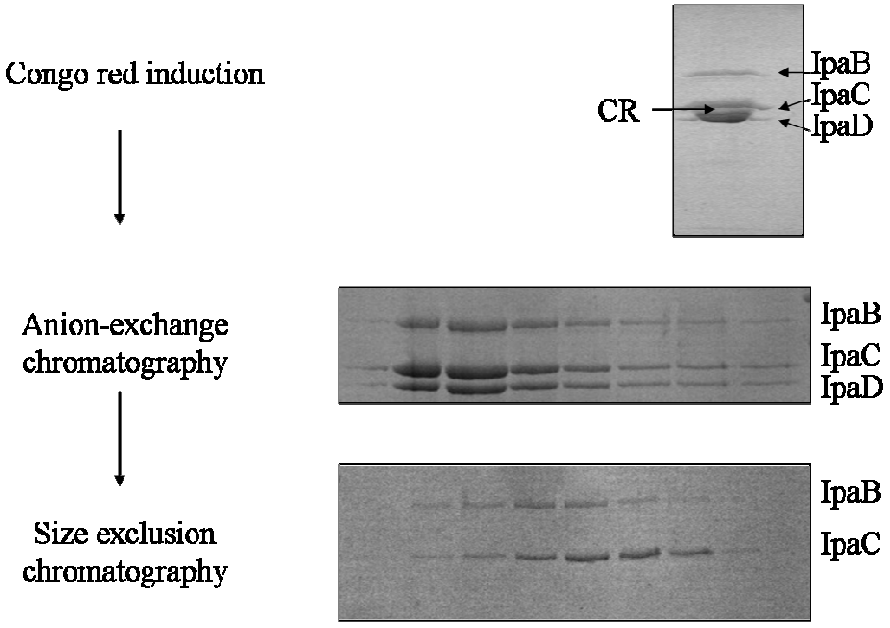

Figure 4.1 Purification of the IpaBC complex from *Shigella flexneri*
IpaB, IpaC and IpaD were prepared from an IpaA IpgD null *Shigella flexneri* strain via Congo red induction (the smear between IpaC and IpaD is Congo red dye). Purification of IpaB, IpaC and IpaD through ion exchange chromatography. Purification of IpaB and IpaC from IpaD through gel filtration column. IpaD is not shown after size exclusion chromatography as it elutes much later at a molecular weight of 37 kDa.

(assuming the complex is globular and spherical in nature). The IpaBC complex migrates at an apparent molecular weight of approximately 190 kDa while free IpaD migrates at a molecular weight of 37 kDa. This migration implies that the IpaBC complex is larger than simply one subunit of IpaB (62 kDa) and one subunit of IpaC (42 kDa). Additional work is needed to determine the exact stiochiometry and composition of the complex; however, this mass potentially implies a IpaB1:IpaC3 complex which correlates with the observed band intensities in the bottom part of Figure 4.1.

Liposome disruption studies

As previously mentioned, both IpaB and IpaC possess hydrophobic regions that have been speculated to be putative transmembrane regions (Mills *et al.,* 1998). Additionally, numerous studies have demonstrated that both IpaB and IpaC delivered by *Shigella* possess the ability to bind to and disrupt red blood cells and liposomes *in vitro* (Clerc *et al.,* 1986). Modified hemolysis assays in which red blood cells (RBC's) were incubated with *Shigella* and then the resulting RBC membranes were purified on a sucrose gradient and probed with anti-IpaB and anti-IpaC antibodies revealed that IpaB and IpaC remain tightly associated with RBC membranes (Blocker *et al.* 1999). In line with these findings, several studies have demonstrated that both IpaB and IpaC have the ability to disrupt and bind artificial membranes *in vitro*, however, there have been no studies to date describing the ability of the IpaBC protein complex to bind or disrupt liposomes (DeGeyter *et al.,* 2000) (Kueltzo *et al.,*

2003) (Harrington *et al.,* 2003) . In order to investigate the ability of the IpaBC pore to disrupt liposomes *in vitro*, unilamelar phospholipid liposomes were synthesized. These liposomes were composed of 50% DOPC, 50% DOPG and 2% cholesterol to very roughly mimic plasma membrane components. In order to monitor liposome disruption in solution, the fluorescent molecule sulforhodamine B (SRB) was used as a probe. SRB was chosen for this assay rather than fluorescein because its fluorescence intensity is independent of pH in the assays used here.

In areas of high concentration many fluorphores, including SRB, exhibit a significant amount of autoquenching (Mach and Middaugh, 1995). Thus, encapsulating fluorescent molecules at high concentrations limit the amount of fluorescence intensity that is detected spectroscopically. If the barrier confining the fluorophore to the high concentration is perturbed, the fluorophores are released into the surrounding solution. Diffusion of the fluorophores into solution results in an increase in fluorescence intensity due to their reduced interaction or local concentration. The rate and amount of fluorescence intensity increase are indicative of how quickly and efficiently the barrier confining the fluorescent molecules is being disrupted (Mach and Middaugh, 2005). By using liposomes to encapsulate SRB, characteristic autoquenching and diffusion priciples can be used to measure the ability of proteins to disrupt lipid bilayers. Whether this occurs by membrane disruption or by pore formation is not measured by this assay as described here (A method to measure pore formation is described later).

Previous work by others in our group has demonstrated that both IpaB and IpaC are able to disrupt liposomes *in vitro* to cause the diffusion of fluorophores into solution (Kueltzo *et al.,* 2003) (Harrington *et al.,* 2003). Additionally, when IpaB and IpaC are bound to the chaperone IpgC, the ability for these proteins to disrupt the liposomes was abolished (Birket *et al.,* 2007). Here we monitor the ability of the IpaBC complex to disrupt liposomes and release fluorophores. SRB-containing liposomes were added to buffer in a quartz cuvette and fluorescence intensity was measured for a short period to establish baseline fluorescence in the absence of purified protein. After establishing a baseline, purified proteins or protein complexes were added to the liposomes in solution and their abilities to disrupt the liposomes was determined by spectroscopically monitoring the increase in fluorescence over time. One percent Trition-X-100 was then added to completely lyse the liposomes and give the maximal increase in fluorescence. As expected, purified IpaB and IpaC were able to disrupt liposomes and cause an increase in fluorescence. Interestingly, the rate and total amount of fluorescence increase was greater when the IpaBC complex was added rather than either purified IpaB or IpaC. These data contrast liposome disruption data for the IpaC/IpgC and IpaB/IpgC complexes, which appear unable to cause liposome distruption (data not shown). Because equal amounts of proteins were added in each case, these data suggest that the IpaBC complex more efficiently causes fluorophore release from the liposomes than the individual translocator proteins (Figure 4.2).

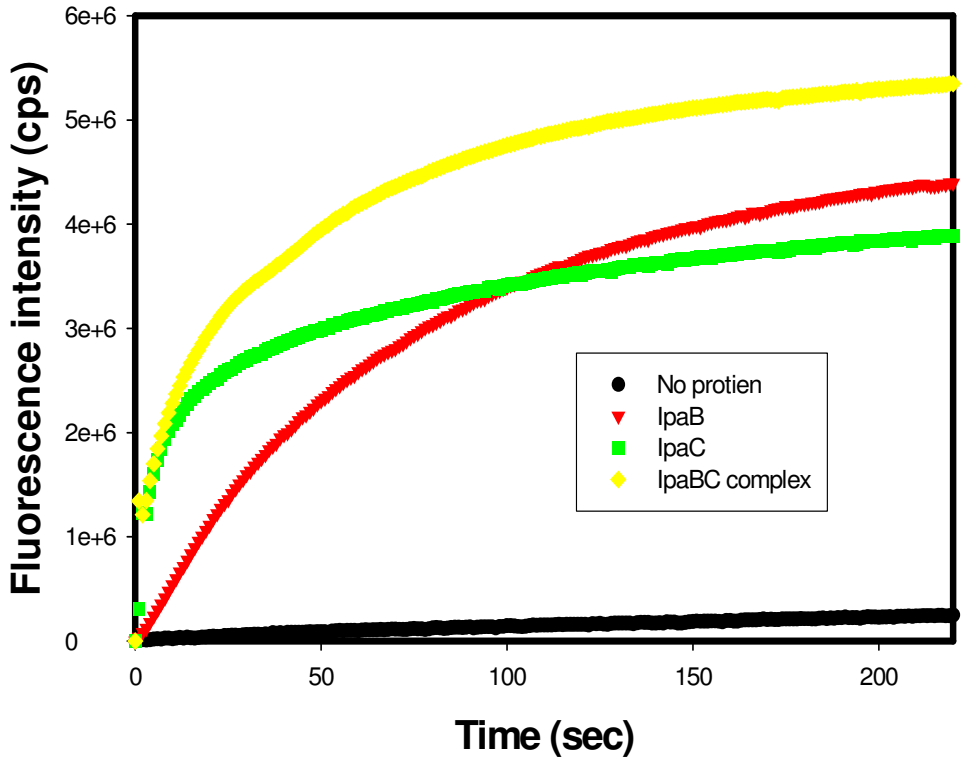

Figure 4.2 Lipid membrane disruption by IpaB, IpaC and IpaBC
Liposomes containing SRB were incubated with IpaB, IpaC and the IpaBC complex and fluorescence was measured over time. Characteristic curves of fluorophore release by protein interaction with the liposome. Each curve is representative of at least three different measurements.

Many cell signaling pathways at the plasma cell membrane are localized to lipid rafts, which contain elevated amounts of cholesterol and specific classes of integral protein membranes. Because the IpaC component of the IpaBC complex has been shown to interact with actin and potentially with Cdc42, it has been proposed that the IpaBC translocon localize to lipid rafts due to interactions with cholesterol (LaFont *et al.,* 2002) (van der Goot *et al.,* 2004). IpaB has been shown to possess cholesterol binding properties which could help to target the IpaBC complex to lipid rafts.

To determine the effect that cholesterol has on the IpaBC pore function, the liposome disruption assays with 50% DOPC:50%DOPG liposomes containing 0% cholesterol and 2% cholesterol (each encapsulating SRB) were constructed. Assays were otherwise conducted exactly as described above. Liposomes containing cholesterol showed a more dramatic increase in fluorescence intensity over time following the addition of the IpaBC complexes than liposomes lacking cholesterol (Figure 4.3). There are potentially several explanations for this observation. It is possible that the IpaBC complex has a greater affinity for liposomes containing cholesterol, resulting in more pore complexes binding the lipsome and thus releasing a higher number of fluorophores. This would be consistent with IpaB's cholesterol binding activity promoting specific interactions with the liposomes. Alternatively, this increased rate of fluorophore release would be caused by the IpaBC complex making more intimate contact with the liposomes (more rapid insertion) due to membrane structure effects of the cholesterol, resulting in a higher rate of fluorophore

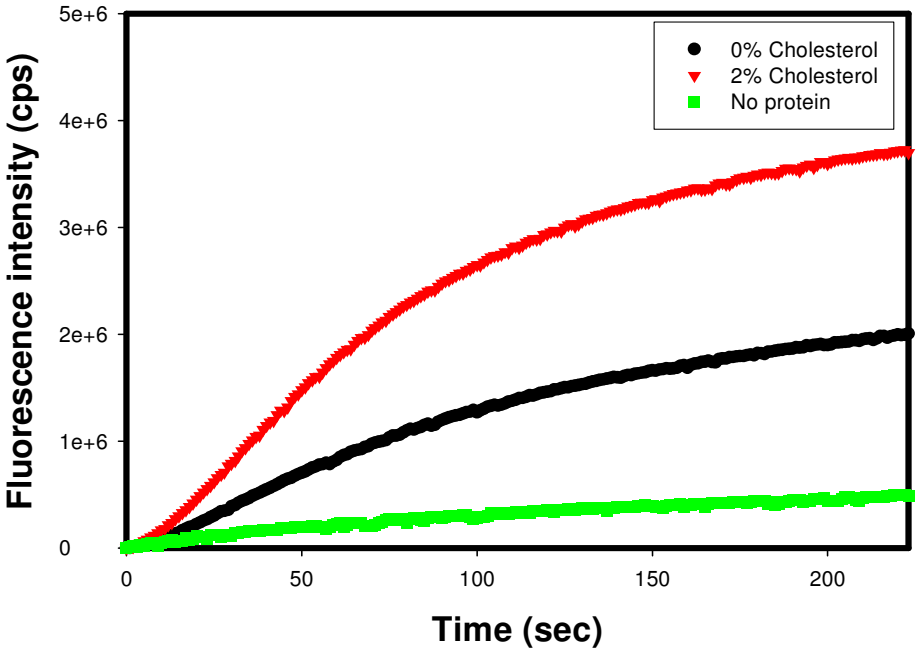

Figure 4.3 IpaBC binds preferentially to cholesterol containing liposomes.
Liposomes containing SRB were incubated with the IpaBC complex and fluorescence was measured over time. The rate and amount of fluorescence by IpaBC is greater in liposomes containing 2% cholesterol (81% release) than liposomes containing no cholesterol (71% release). Curves are representative of at least three separate measurements. Liposomes in PBS only (no protein) are included as a negative control.

release. Ultimately, it appears that the addition of cholesterol to the lipid mixture enhances the IpaBC translocon complex's ability to disrupt lipid membranes.

It is important to note that small increases in cholesterol have been observed to enhance the translocon's ability to disrupt liposomes, however, this enhancement may have an upper limit. In liposome disruption assays where liposomes contain equal concentrations of DOPC and DOPG and 5% cholesterol IpaBC ability to disrupt liposomes is similar to rates of liposomes possessing 2% cholesterol. In the same assay, where liposomes contain 20% cholesterol, lipsome disruption occurs at a rate lower than 2% containing liposomes (observation, data not shown). Additional investigation will have to occur to determine if high amounts of cholesterol are inhibitory to IpaBC binding, however these later observations may be consistent with cholesterol physical effects on the liposomes having influence on the IpaBC complex disruption of those liposomes. Alternatively, at very high cholesterol concentrations, it is possible that small amounts of free sterol may be competing with the liposomes for binding to IpaB.

Biophysical characterization of the IpaBC pore

To investigate changes that may have occurred in the IpaB and IpaC secondary structure upon IpaBC complex formation, circular dichroism was employed to monitor secondary structure of purified IpaB, IpaC and the IpaBC complex. Both far UV spectra and thermal melting spectra of the purified proteins show that upon binding to one another, IpaBC complex undergoes a change in

secondary structure that coincides with an increase in thermal stability of the proteins (Figure 4.4 and Table 4.1). The incorporation of IpaB and IpaC into IpaBC complexes appear to be accompanied by an increase in the α-helical state of the proteins. Thermal stability is monitored by following the CD signal at 222 nm as temperature is increased to determine the movement of α-helical structures to a more disordered state. The binding of IpaB and IpaC to each other appears to induce a more structured and more stable protein than that of either protein alone (Table 4.1).

Pore Formation

Previously, Blocker *et al.* have used osmotic protection assays in conjunction with contact-mediated hemolysis assays to estimate the inner diameter of the IpaBC translocon complex (Blocker *et al.,* 1999). Erythrocyte hemolysis assays are routinely used to determine the efficiency of translocon formation by *S. flexneri* in RBC membranes (Clerc *et al.,* 1987). Bacterial cultures are incubated with RBCs and then hemolysis is determined by measuring the absorbance of free hemoglobin. In this assay, pore formation by the TTSA in the RBC membrane leads to osmotic disequilibrium and eventually lysis of the red blood cell. In order to estimate the inner diameter of the pore, osmotic protection assays were carried out by coupling hemolysis with the addition of osmoprotectants of various sizes to prevent cell lysis. Osmoprotectants larger than 26 Å were able to block the pore and prevent osmotic shock and cell lysis, thereby suggesting that this is the approximate size of the translocon pore (Blocker *et al.,* 1999).

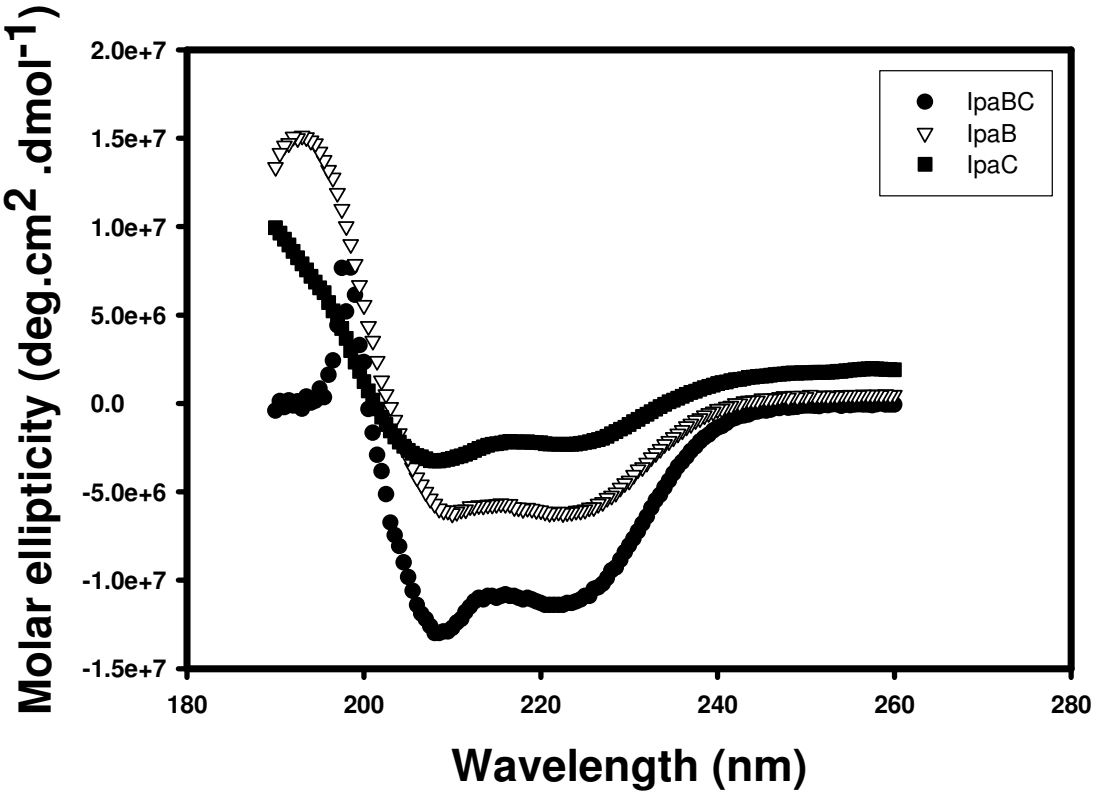

Figure 4.4 Far UV CD spectra of purified IpaB, IpaC and the IpaBC pore. Far UV spectra and melting temperatures were monitored by circular dichroism. CD spectra were monitored from 190 nm to 280 nm, while T_m were determined by monitoring the transition of spectra at 222 nm from α-helical structure to disordered state.

Protein	Melting Temperature (Tm) ± SE, °C
IpaB	51.6 ± 0.0
IpaC	45.5 ± 0.3
IpaBC	56.7 ± 0.4

Table 4.1 Thermal unfolding temperatures of purified IpaB, IpaC and IpaBC complex as monitored by CD.
Proteins were monitored at 222 nm over increasing temperature to determine transitions from α-helical conformations to a state of disorder. Melting temperatures were determined by the midpoint of a fitted sigmoidal curve.

To relate these past findings to the activity of the purified IpaBC complex, an alternative approach was taken to determine whether there is pore formation in artificial liposomes. Liposomes were constructued using 25% DOPC:75% DOPG and encapsulating fluorescently labeled dextrans with a hydrodynamic radius ranging from less than 1.0 nm to approximately 3.5 nm. Despite their large and varied sizes, these molecules also exhibit autoquenching with respect to their fluorescence when entrapped at high concentrations in liposomes. Liposome disruption assays were conducted as previously described above and fluorescence intensity was again measured spectroscopically (Figure 4.5). Those liposomes containing dextrans of a hydrodynamic radius of 2.2 nm or less released the highest amounts of fluorescence (25-28%) while those with a hydrodynamic radius of 3.5 nm released significantly less fluorescence (8%) suggesting the pore has an upper limit between 2.2 nm and 3.5 nm (A.H. Harrington, unpublished data). These data are consistent with previous estimations of pore inner diameter and they show the IpaBC complex can form pores in liposomes *in vitro* (Harrington *et al.,* 2005).

To further determine the physical dimensions of the pore complex, purified IpaBC complexes were sent to Dr. Stefan Bossmann at Kansas State University to analyze using atomic force microscopy (AFM). Dr. Bossman's current work includes pore formation by the *Mycobacterium smegmatis* porin, MspA. AFM is a scanning probe microscopy method capable of resolution at the nanometer scale.

IpaBC protein samples were spin-coated onto P(NIPAM/Acrylic acid) coated chips and were then imaged through "tapping mode." As the canteliver and tip are

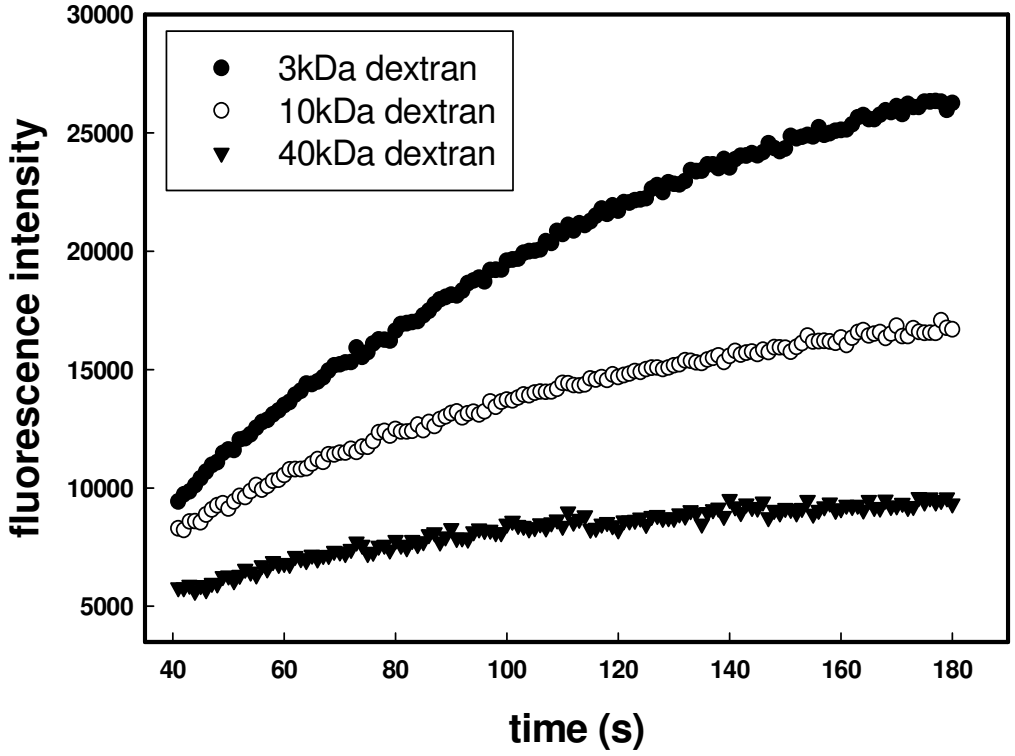

Figure 4.5 IpaBC pore formation is reflected through size exclusion.
Three different sized dextrans were encapsulated in liposome bilayers and incubated with equal concentrations of IpaBC complex. Three kDa dextrans have a hydrodynamic diameter of less than 1 nm and release 28% of dextrans. Ten kDa dextrans have a hydrodynamic diameter of 1.8 to 2.2 nm and release 22% of dextrans, while 40 kDa dextrans have a diameter of approximately 3.5 nm and release 8% dextrans (A.H. Harrington, unpublished data).

tapped across the sample they are able to provide a topographical picture of the slide's surface (Engel, 2002). AFM data received from Dr. Bossmann show that IpaBC complex is consistently uniform in size (Figure 4.6 and Figure 4.7). Perhaps more importantly, the IpaBC complex forms pores within the acrylamide coating with a corrected inner diameter of 3.5 nm ± 0.5 nm. The outer diameter of the pore complex was also determined to be 13.5 nm ± 1.5 nm (data not shown). These data correlate well with the liposome studies previously shown in this Chapter for inner pore diameter in addition to unpublished dynamic light scattering data for the pore's outer diameter (W.D. Picking, unpublished data).

Discussion

Unlike most of the proteins from the *S. flexneri* TTSS studied in our lab, we purify the IpaBC complex from the pathogen rather than producing recombinant protein in *E. coli.* Because we can purify the protein from its native environment, it is more likely to form a native complex. Utilizing the small molecule dye Congo red, we can mimic host cell interaction and induce the secretion of effector proteins into the extracellular milleu. By using an *ipaA/ipgD* null *S. flexneri* strain, we can effectively purify soluble IpaBC translocon complex for detailed study.

Circular dichorism data show that binding of the translocator proteins to each other results in an increased state of protein organization. This conformational effect probably is more associated with IpaC since it has a high degree of unstructured component when alone in solution. The thermal melting temperature of the IpaBC

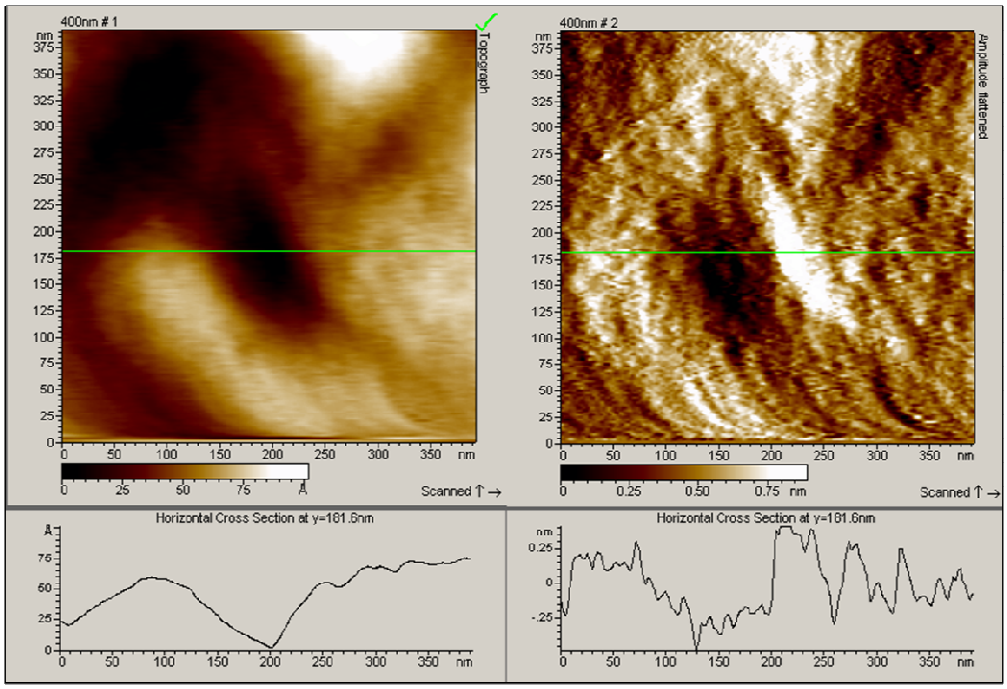

Figure 4.6 Atomic force microscopy of the IpaBC pore complex. IpaBC complexes were spin-coated into acrylamide coated slides and measurements were taken using atomic force microscopy. Horizontal cross-sections were measured through "tapping" methods across the surface of the slide (green line). Images were taken at a resolution of 400 nm. Images are courtesy of Dr. Stefan Bossmann, University of Kansas.

A.

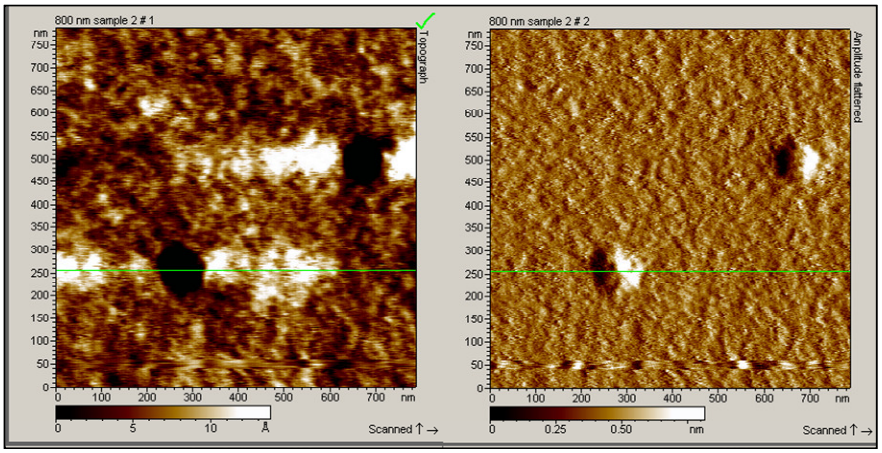

B.

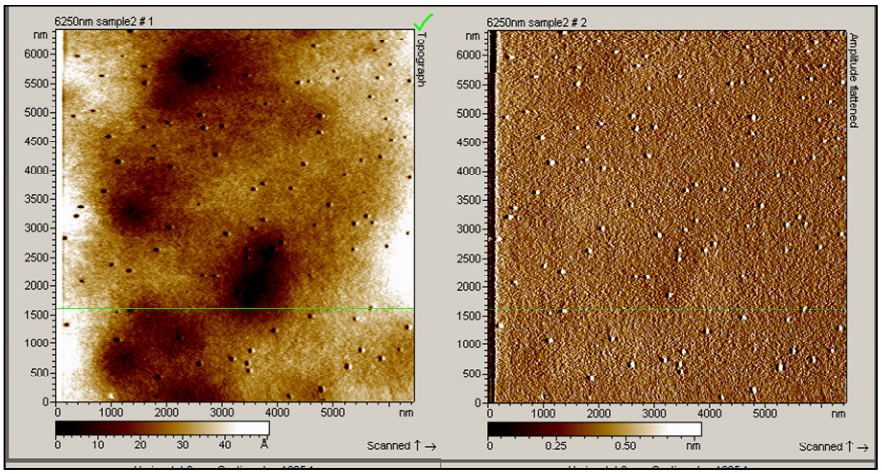

Figure 4.7 Additional AFM images depicting IpaBC complexes.
The AFM figures above depict IpaBCprotein complexes of similar sizes and shapes. A. Image at 800 nm, image on the left is raw data while image on the right is refined. B. Pore complexes imaged at 6250 nm, left image is raw data, while the right frame is refined.

complex is higher than either IpaB or IpaC alone, suggesting that upon translocon formation, the protein components are stabilized. As previously demonstrated, and similar to other type III translocator proteins such as PopB and PopD in *Pseudomonas aeruginosa* and YopB and YopD in *Yersinia* spp., the IpaB and IpaC proteins are capable of individually interacting with phospholipid membranes. Here we show that not only is the IpaBC complex also capable of this interaction, but it also appears that this interaction is enhanced for the IpaBC complex relative to IpaB and IpaC individually. These data correlate with CD spectroscopic analyses, strengthening the proposal that upon IpaBC binding the two proteins undergo a conformational change that enhances membrane binding function and protein stability. This change may be related to function.

It has been well documented that lipid rafts play an important role in cell signaling processes. Efficient invasion by in *Salmonella* and *Shigella* has been shown to require the presence of cholesterol. It has also been demonstrated that IpaB is a cholesterol binding protein. With this in mind, it could be deduced that cholesterol plays an important role in translocon insertion into the host cell membrane. Our liposome assays show that not only does the IpaBC complex bind to cholesterol-containing liposomes, but the IpaBC complex may have a greater affinity for membranes containing cholesterol or that cholesterol may induce a conformational change in the IpaBC complex that allows the complex to insert more efficiently into membrane bilayers. The ability for IpaB to behave as a cholesterol binding protein makes it attractive to speculate that this activity increases the affinity for the IpaBC

complex for liposomes that have a cholesterol component. Interestingly, very high concentrations of cholesterol seemed to reverse this trend.

Circular dichroism shows that the *Shigella* IpaBC complex contains a high degree of α-helicity and that the pore complex is more thermally stable than either protein alone. Biophysical analyses also provided insight into the structural dimensions of the IpaBC complex. Liposome assays suggest that the inner diameter of the IpaBC complex has an upper limit of over 2.2 nm but well under 3.5 nm. Supporting data were obtained from AFM analyses.

The data presented here touch on some of the biophysical aspects of the IpaBC translocon but there are still a number of aspects of the *S. flexneri* translocon that warrant investigation. To date, there the exact stoichiometry and subunit composition of the IpaBC complex are unknown. Additional biophysical methods such as dynamic light scattering and ultracentrifugation could be used to investigate some of the structural unknowns that remain for the IpaBC complex.

CHAPTER 5

Tyrptophan Scanning Mutagenesis of IpaB

Introduction

IpaB and IpgC interactions

As described in Chapters 1 and 4, IpaB is a large effector molecule that is part of the *Shigella flexneri* type III secretion system. IpaB possesses distinct functional roles within *Shigella* type III secretion, including the ability to direct apoptosis in macrophages, bind and insert into lipid membranes and, with IpaC, form a translocon complex that inserts as a pore into targeted host cell membranes to direct the entry of other effector proteins into the host cell cytoplasm (Menard *et al.,* 1994b) (Zychlinsky *et al.,* 1994) (Blocker *et al.,* 1999) . Due to IpaB's large molecular size (62 kDa) and hydrophobicity, structural information of the protein is limited. Based on secondary structure and structure-function analyses several key regions of IpaB have been described (Figure 5.1). IpaB possesses a N-terminal coil, a hydrophobic putative transmembrane region and a predicted large C-terminal coil. Structure function analyses by Guichon *et al.,* have determined that large deletions within the N-terminus resulted in loss of protein expression; while large deletion mutantions within the C-terminus of IpaB were expressed, but invasion, cell cytotoxicity and phagosomal escape were diminished or abolished. Additionally, most small internal deletions within the putative transmembrane region resulted in protein function

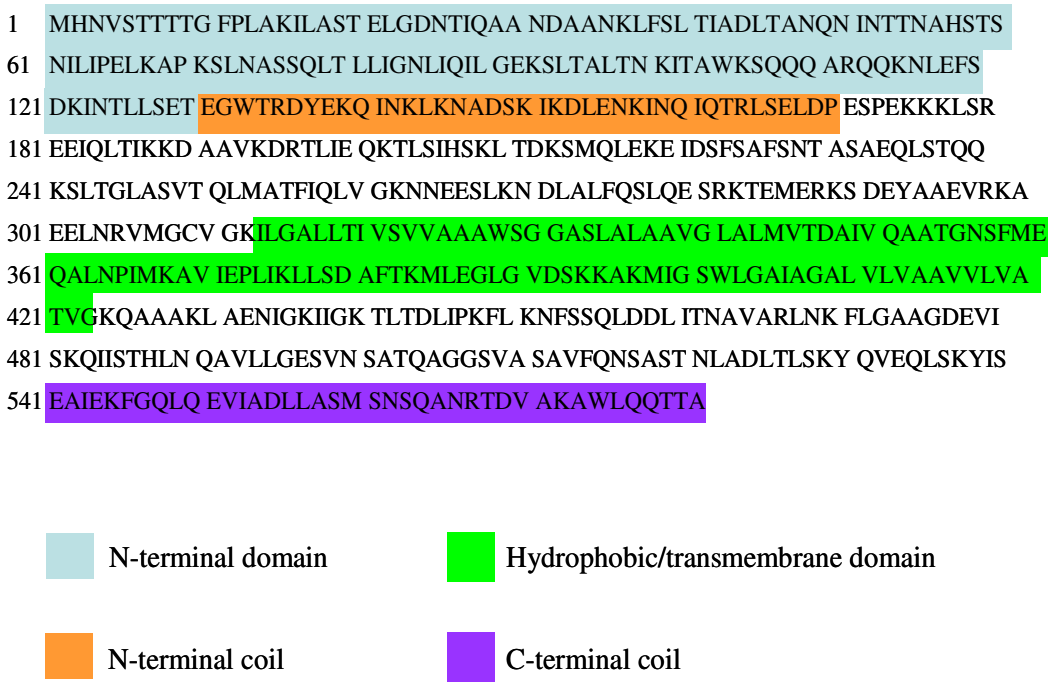

Figure 5.1 Schematic diagram of regions within IpaB.
Residues 1-130 are the N-terminus, while residues 130-170 are predicted to be an N-terminal coil. Residues 310-420 are hydrophobic domains. Amino acids 540-580 make up a C-terminal coil.

similar to wild type (Guichon *et al.*, 2001). There were two exceptions to this, including a deletion encompassing the seven residues before, and three residues within, the transmembrane region (amino acids 307-313) and alternatively, a deletion of amino acids 410-417 from the transmembrane region (Guichon *et al.,* 2001). The mutant lacking amino acids 307-316 was expressed similarly to wild-type levels, while the mutant lacking residues 410-417 was poorly expressed in *Shigella* (Guichon *et al.,* 2001). This suggests that the transmembrane region of IpaB may serve multiple functions in type III secretion.

Prior to secretion by the TTSS, IpaB resides in the bacterial cytoplasm bound to the chaperone IpgC (Menard *et al.,* 1994b). Chapters 1 and 3 describe the importance of IpgC's role in *S. flexneri* type III secretion. IpgC is a class II chaperone that associates individually with IpaB and IpaC, performing several functions within the type III secretion system of *Shigella flexneri*. IpgC's association with IpaB and IpaC prevents premature association of IpaB with IpaC which would result in degradation of the translocator components within the bacterial cytoplasm. IpgC is also proposed to hold IpaB in a secretion competent state for passage through the needle apparatus of the TTSS (Page *et al.,* 1999).

Little research has been devoted to understanding the IpaB/IpgC interaction or the structural influences these proteins impart on each other. In this Chapter, we investigate the influence of IpgC binding on IpaB using spectroscopic techniques. Members of our lab have previously used tryptophan scanning mutagenesis as an efficient tool to determine how different regions of IpaC are influenced by IpgC

binding. Here we have initiated use of the same technique to determine regions of IpaB influenced by IpgC binding.

Results

Strain Construction and Protein Purification

Previous work by Harrington *et al.* and Birket *et al.* utilized Trp scanning mutagenesis to determine how liposome and IpgC binding influenced the structure and the microenvironment of different IpaC regions (Harrington et al, 2005) (Birket *et al.,* 2007). Because of the intrinsic environmental sensitivity of the indole group of tryptophan, Trp scanning mutagenesis can be a practical tool for probing the local environment of Trp residues in single-Trp containing proteins. Trp fluorescence is directly influenced by the polarity of its surroundings and can be used to determine changes influenced by protein binding.

In order to accurately characterize proteins using tryptophan fluorescence, proteins must only carry a single Trp residue. In previous Trp scanning mutagenesis experiments, key IpaC residues were mutated to Trp to construct a library of single-Trp containing IpaC mutants. Because wild-type IpaC does not possess a natural Trp residue, point mutations were easily made to strategic regions of IpaC. In contrast, wild-type IpaB contains a single Trp residue at position 105 (Figure 5.2). Conveniently, this natural Trp residue can be used to characterize the N-terminal region of IpaB; however, to create subsequent IpaB single-Trp mutants this residue had to first be removed. IpaB Trp mutants were thus constructed by creating first a

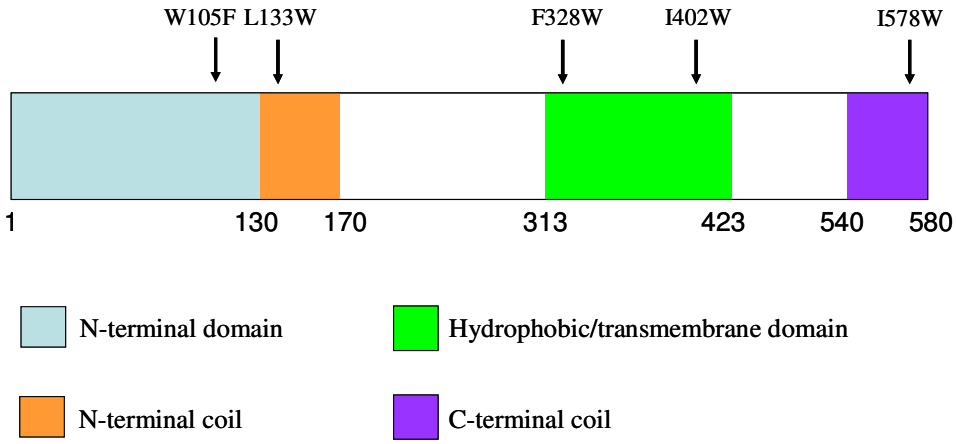

Figure 5.2 Position of tryptophan mutations within IpaB.
A natural Trp residue is located at position 105. In order to make single Trp-containing mutants all mutants were constructed by replacing the natural Trp at 105 with Phe and then used as a template to construct subsequent Trp mutations located at positions 133, 328, 402 or 574. Key structural or functional regions are highlighted.

Trp knockout mutant in which W105 was converted to a phenyalanine. This knockout was then used as a template to create additional Trp-containing IpaB mutants.

To characterize regions of IpaB influenced by IpgC binding, several key regions were chosen at which new Trp residues could be introduced: position 133 in the predicted N-terminal coil; positions 328 and 402 in the hydrophobic/putative transmembrane domain; and at position 574 in the putative N-terminal coil (Figure 5.2). The primers used are given in Table 5.1. All the Trp mutants were generated using the point mutation W105F so that all mutants contained a single Trp residue, resulting in double mutants containing W105F and a single-Trp mutation. The removal of the natural Trp at 105 had no effect on IpaB invasion or hemolysis (Table 5.2).

IpaB Trp mutants were created utilizing site-directed mutagenesis (Picking *et al.,* 1996). Primers used to construct Trp mutants are listed in Chapter 1 as Table 2.1 and here as Table 5.1. Hydrophobic amino acids with bulky sidechains, such as leucine and isoleucine, were targeted for Trp mutagenesis to minimize changes to protein structure that might reduce IpaB function.

Like IpaC/IpgC, IpaB can be purified as a soluble complex with IpgC. IpaB mutants were co-expressed with His-tagged IpgC and recombinant proteins were initially purified from Tuner (DE3) *E. coli* using Ni^{+} affinity chromatography. Peak fractions were pooled and the resulting IpaB/IpgC complex was seperated from free IpgC by size-exclusion chromatography. In contrast to the IpaC/IpgC complex,

Mutant	Primer Names	Sequence (3'-5')
W105F	B50f	GAGAGAGAGATTTAAATCCCAGCAACAGGCAAG
	B51r	GAGAGAGAGATTTAAATGCAGTAATTTTATTTGTTAATG
L133W[a]	B53f	GAGAGAGAGACGCGTGACTATGAAAAACAAATTAATAA
	B54r	GAGAGAGAGACGCGTCCATCCTTCAGTTTCAGATAGAA
F328W[a]	B57f	GAGAGAGAGGCCGCTTGGTCTGGAGGAGCCTCTCTA
	B58r	GAGAGAGAGGCGGCCGCAACAACACTAACGATAGT
I402W[a]	B59f	GAGAGAGAGGCCGGCGCTCTTGTCCTAGTT
	B60r	GAGAGAGAGGCCGGCGATTGCCCCCAGCCAAGAGCCAATCTATTTGGCTT
I574W[a]	B61f	GAGAGAGAGCTGCAGCAAACTACTGCTTGAGGC
	B62r	GAGAGAGAGCTGCAGCCATGCTTTGCAACATCAGTT

Table 5.1 Table of primers for IpaB tryptophan scanning mutants
[a]Mutations after 105 are double mutants containing W105F and the indicated mutation.

IpaB/IpgC cannot be separated by lowering the solution pH, suggesting a different set of molecular interactions involved in this chaperone binding event. Previous work by Hume *et al.* has determined that detergent can be used to purify IpaB from *E. coli,* in the absence of IpgC (Hume *et al.,* 2003). The IpaB/IpgC complex was therefore incubated with 2% n-octyl-poly-oxyethylene (OPOE) detergent, which was found to release the IpaB from IpgC. The proteins were then separated using Ni^+ affinity chromatography where IpaB elutes in the flow through while His-tagged IpgC and remaining IpaB/IpgC complexes are bound to the column (Figure 5.3).

IpaB Tryptophan Mutant Characterization

Most of the Trp mutations introduced here resulted in little change in protein thermal stability, or the secretion, invasivness or hemolytic activity of the mutant IpaB when it is made in *S. flexneri ipaB* null strain, SF620 (Tables 5.2 and 5.3). Interestingly, the two Trp mutations made within the hydrophobic/transmembrane region of IpaB appear to behave differently from one another. When made in SF620, IpaB possessing the F328W mutation appeared to retain wild-type function, while I402W, which is also found in the transmembrane region, appears to lose its ability to invade Henle 407 cells and is no longer hemolytic. Additionally, i*paB* is expressed at reduced quantities in the I402W mutant (Figure 5.3). Expression levels of *ipaB* and *ipgC* all IpaB Trp mutants are represented in Figure 5.3.

Because CD spectroscopy provides data about global secondary structure, one would predict that the values in Table 5.3 would provide the same thermal unfolding

temperature unless a point mutation had a significant effect on overall protein structure. Thermal melting temperatures of these proteins range from 59.2 ºC to 64.2 ºC. Although values in Table 5.3 are relatively close to each other, additional CD measurements would be needed to confirm these data. Further melts involving Trp

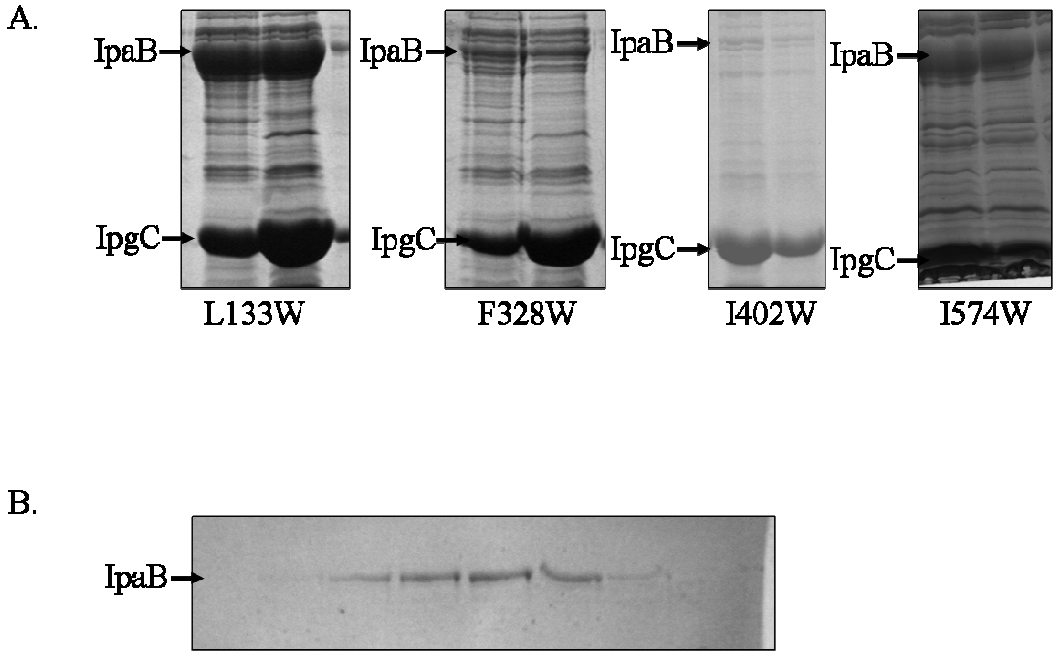

Figure 5.3 Expression and protein purification of IpaB Trp mutations.
A. IpaB Trp mutants were co-expressed in *E. coli* with His-tagged IpgC. Proteins were purified through affinity chromatography. Free IpgC was separated from the complex through size exclusion chromatography (not shown).
B. IpaB/IpgC complexes were separated by incubating with OPOE and then were loaded onto an Ni^{+} affinity column. Free IpaB eluted in the flow through fractions while remaining IpaB/IpgC complexes and free IpgC eluted in 1M imidazole (not shown).

fluorescence would be able to provide local information since Trp fluorescence is influenced by local environment rather than global protein structure.

Mutant	Relative Hemolysis (%) ± SD	Relative Invasion (%) ± SD
IpaB (wt)	100	100
W105F	95 ± 15	89 ± 8
W105F/L133W	94 ± 9	83 ± 20
W105F/F328W	103 ± 12	86 ± 8
W105F/I402W	1 ± 0	1 ± 0
W105F/I574W	105 ± 14	77 ± 4

Table 5.2 Relative invasion and hemolysis of IpaB Trp mutants.
Invasion and hemolysis are relative to IpaB complement *Shigella flexneri* strains.

Protein[a]	Melting Temperature (T_m), °C IpaB/IpgC complexes
IpaB (wt)	64.1
W105F/L133W	59.2
W105F/F328W	62.9
W105F/I402W	TBD
W105F/I574W	64.2

Table 5.3 Thermal melting temperatures of purified IpaB and IpaB Trp mutants.

[a]Melting temperature for IpaB varies in this Chapter than previously reported in Chapter four. Thermal unfolding was monitored on a different CD instrument and may account for variation, all IpaB Trp mutants were measured at the same time as the above IpaB on the same instrument. Melting temperatures are an average of at least three spectra.

Acquisition of Tryptophan Emission

In order to determine the polarity of the microenvironment of the Trp residues in IpaB, fluorescence emission maxima were determined for each purified single-Trp containing IpaB/IpgC complex and the corresponding free form of the IpaB mutant. Trp residues were excited at a wavelength of 290 nm and Trp emission maxima were determined using a scanning fluorescence spectrophotometer. Trp emission maxima that shift to a shorter wavelength (blue shift) upon IpaB binding to IpgC suggest movement of that Trp residue into a more nonpolar environment. Movement of emission maxima to a longer wavelength (red shift), are indicative of movement into a more polar environment (Mach and Middaugh, 1995). The acquisition of trypyophan fluorescence maxima is still in progress. Preliminary results show that most complexes exhibit significant red shifts upon IpgC binding, suggesting that IpgC does influence changes in the local environment in key regions of IpaB (Table 5.4 and data not shown). A red shift upon IpgC binding indicates movement of the Trp residues into a more polar environment, meaning the Trp residues are more exposed to the surrounding solvent or the protein may be in a more unfolded state when bound to IpgC. More work on these experiments will have to continue to fully and

accurately characterize the influences of IpgC binding on IpaB residues at positions 105, 133, 328 and 574. Because of poor protein expression levels of the I402W mutant, additional experiments will not be continued for this protein.

Protein	Emission maximum (E_m), nm with chaperone IpgC	Emission maximum (E_m), nm without chaperone IpgC	Change in emission maximum (ΔE_m), nm with chaperone IpgC
IpaB	TBD	TBD	TBD
W105W/L133W	341.0	337.1	+ 3.6
W105W/F328W	332.0	TBD	TBD
W105W/I402W	TBD	TBD	TBD
W105W/I574W	TBD	TBD	TBD

Table 5.4 Tryptophan fluorescence emission maxima for IpaB Trp mutants. Purified IpaB and IpaB/IpgC complexes were excited at 290 nm and emission maxima were determined spectroscopically. TBD, to be determined.

Discussion and Future Plans

Trp scanning mutagenesis has provided a useful tool in determining regions of IpaC influenced by association with IpgC and liposomes. In this study we are usin the same technique to investigate how regions of IpaB are influenced by chaperone binding as well. Single Trp mutants of IpaB displayed relatively little change in the phenotype when made in *Shigella* with the exception of the substitution of Trp for Ile at position 402 in the hydrophobic putative transmembrane region of IpaB. The presence of IpgC in I402W protein purification suggests that IpaB is expressed, because in the absence of IpaB being made IpgC must be recovered from inclusion bodies rather than the bacterial cytoplasm. If IpaB had not been made at all, IpgC recovery would require an alternative means of purification (personal observation). In contrast, a similar mutation to the hydrophobic region (F328W) had little impact the phenotype of the protein. As mentioned earlier in this Chapter, previous structure function mutational analyses revealed that small deletions in the of the first half of the putative transmembrane domain (including 328) has little impact on the function of the protein, as compared to wild type, while deletion within the second half of the putative transmembrane region resulted in poor expression of the protein (Guichon *et al.,* 2001). This would be consistent with our observation that the I402W mutation

may destabilize IpaB, however, in our case there has not been a deletion introduced but rather a substitution.

If IpaB is misfolded and only able to transiently associate with IpgC, it may be quickly targeted for degradation in the *Shigella* and/or *E. coli* cytoplasm. This, taken together with data previously reported on IpaB stability, suggests that the transmembrane region plays a significant role in IpgC binding and/or IpaB structural stability. It is possible that the I402W mutation disrupts the chaperone binding, thus targeting IpaB for degradation. Alternatively, the I402W mutation may result in structural changes that prevent proper folding of IpaB.

Initial findings suggest that residues 105, 133, 328 and 574 are influenced by IpgC binding (preliminary data, not shown). These areas of IpaB appear to be red shifted upon IpgC binding suggesting movement of the Trp residues into a more polar environment. This would suggest that IpgC somehow increases the exposure of these residues to the surrounding solution, possibly by holding IpaB in a more unfolded state. As previously stated, IpaB possess the ability to bind to IpgC, IpaC and liposomes. It is evident that IpgC works to prevent key binding regions of IpaB from prematurely associating with IpaC and from associating with the interior face of the bacterial plasma membrane. To determine whether IpgC physically wraps around key regions of IpaB and/or induces conformational changes that prevent exposure of these IpaB regions to the surrounding solution will require additional investigation.

The above work has demonstrated that like IpaC, a library of IpaB tryptophan mutants can be constructed to determine the influence of binding partners on IpaB

structure or to determine which regions of IpaB are involved in these interactions. The majority of these tryptophan mutations resulted in the purification of soluble IpaB/IpgC complexes and did not significantly affect IpaB structure, pore formation or epithelial cell invasion. Future work in this area will include finishing characterization of the Trp emission from the introduced IpaB Trp mutants. Additional mutants could be made and added to the library to more closely examine IpaB structure and function. Previous work by members of our lab has used IpaC Trp mutants to characterize liposome interactions with IpaC in addition to IpaC/IpgC binding. Because IpaB also possess the ability to bind liposomes, the IpaB Trp mutants could be used to monitor these interactions as previously described by Harrington *et al.*

Local structural changes in the IpaB could also be determined using IpaB Trp mutants. Unlike CD spectroscopy, which monitors global secondary structure, fluorescence spectroscopy can be used to monitor secondary structure in the local environment of the Trp residues (Birket *et al.*, 2007). Fluorescence intensity spectra can be used to monitor the stability of a specific region of IpaB rather than the entire protein, more accurately describing the types of effects that binding has upon IpaB.

RESOURCES CITED

Adam, T., Arpin, M., Prevost, M. C., Gounon, P., and Sansonetti, P. J.,Cytoskeletal rearrangements and the functional role of T-plastin during entry of *Shigella flexneri* into HeLa cells *J Cell Biol* **129** (2), 367 (1995).

Adam, T., Giry, M., Boquet, P., and Sansonetti, P.,Rho-dependent membrane folding causes *Shigella* entry into epithelial cells *Embo J* **15** (13), 3315 (1996).

Alto, N. M., Shao, F., Lazar, C. S., Brost, R. L., Chua, G., Mattoo, S., McMahon, S. A., Ghosh, P., Hughes, T. R., Boone, C., and Dixon, J. E.,Identification of a bacterial type III effector family with G protein mimicry functions *Cell* **124** (1), 133 (2006).

Aubert, D.F., Flannagan, R.S., Valvano, M.A. A novel sensor kinase-response regulator hybrid controls biofilm formation and type VI secretion system activity in Burkholderia cenocepacia *Infect Immun* **76** (5), 1979 (2008).

Bahrani, F. K., Sansonetti, P. J., and Parsot, C.,Secretion of Ipa proteins by *Shigella flexneri*: inducer molecules and kinetics of activation *Infect Immun* **65** (10), 4005 (1997).

Blocker, A., Gounon, P., Larquet, E., Niebuhr, K., Cabiaux, V., Parsot, C., and Sansonetti, P.,The tripartite type III secreton of *Shigella flexneri* inserts IpaB and IpaC into host membranes *J Cell Biol* **147** (3), 683 (1999).

Blocker, A., Holden, D., and Cornelis, G.,Type III secretion systems: what is the translocator and what is translocated? *Cell Microbiol* **2** (5), 387 (2000).

Blocker, A., Jouihri, N., Larquet, E., Gounon, P., Ebel, F., Parsot, C., Sansonetti, P., and Allaoui, A.,Structure and composition of the *Shigella flexneri* "needle complex", a part of its type III secreton *Mol Microbiol* **39** (3), 652 (2001).

Buttner, D. and Bonas, U.,Port of entry--the type III secretion translocon *Trends Microbiol* **10** (4), 186 (2002).

Clerc, P., Baudry, B., and Sansonetti, P. J.,Plasmid-mediated contact haemolytic activity in Shigella species: correlation with penetration into HeLa cells *Ann Inst Pasteur Microbiol* **137A** (3), 267 (1986).

Davis, R., Marquart, M. E., Lucius, D., and Picking, W. D.,Protein-protein interactions in the assembly of *Shigella flexneri* invasion plasmid antigens IpaB and IpaC into protein complexes *Biochim Biophys Acta* **1429** (1), 45 (1998).

De Geyter, C., Vogt, B., Benjelloun-Touimi, Z., Sansonetti, P. J., Ruysschaert, J. M., Parsot, C., and Cabiaux, V.,Purification of IpaC, a protein involved in entry of *Shigella flexneri* into epithelial cells and characterization of its interaction with lipid membranes *FEBS Lett* **400** (2), 149 (1997).

De Geyter, C., Wattiez, R., Sansonetti, P., Falmagne, P., Ruysschaert, J. M., Parsot, C., and Cabiaux, V.,Characterization of the interaction of IpaB and IpaD, proteins required for entry of *Shigella flexneri* into epithelial cells, with a lipid membrane *Eur J Biochem* **267** (18), 5769 (2000).

DuPont, H. L., Levine, M. M., Hornick, R. B., and Formal, S. B.,Inoculum size in shigellosis and implications for expected mode of transmission *J Infect Dis* **159** (6), 1126 (1989).

Espina, M., Olive, A. J., Kenjale, R., Moore, D. S., Ausar, S. F., Kaminski, R. W., Oaks, E. V., Middaugh, C. R., Picking, W. D., and Picking, W. L.,IpaD localizes to the tip of the type III secretion system needle of Shigella flexneri *Infect Immun* **74** (8), 4391 (2006).

Fath, J. R. and Kolter, R.,ABC Transporters: Bacterial Exporters *Microbiol Rev* **57**, 995 (1993).

Formal, S. B., Hale, T. L., and Sansonetti, P. J.,Invasive enteric pathogens *Rev Infect Dis* **5 Suppl 4**, S702 (1983).

Guichon, A., Hersh, D., Smith, M. R., and Zychlinsky, A.,Structure-function analysis of the *Shigella* virulence factor IpaB *J Bacteriol* **183** (4), 1269 (2001).

Handa, Y., Suzuki, M., Ohya, K., Iwai, H., Ishijima, N., Koleske, A. J., Fukui, Y., and Sasakawa, C.,Shigella IpgB1 promotes bacterial entry through the ELMO-Dock180 machinery *Nat Cell Biol* **9** (1), 121 (2007).

Hakansson, S., Bergman, T., Vanooteghem, J. C., Cornelis, G., and Wolf-Watz, H.,YopB and YopD constitute a novel class of Yersinia Yop proteins *Infect Immun* **61** (1), 71 (1993).

Harper, J. R. and Silhavy, T. J., in *Principles of Bacterial Pathogenesis*, edited by E. A. Groisman (Academic Press, New York, NY, 2001), pp. 43.

Harrington, A. T., Hearn, P. D., Picking, W. L., Barker, J. R., Wessel, A., and Picking, W. D.,Structural characterization of the N terminus of IpaC from *Shigella flexneri Infect Immun* **71** (3), 1255 (2003).

Harrington, A., Darboe, N., Kenjale, R., Picking, W. L., Middaugh, C. R., Birket, S., and Picking, W. D.,Characterization of the Interaction of Single Tryptophan Containing Mutants of IpaC from *Shigella flexneri* with Phospholipid Membranes *Biochemistry* **45** (2), 626 (2006).

Hayward, R. D. and Koronakis, V.,Direct nucleation and bundling of actin by the SipC protein of invasive Salmonella *Embo J* **18** (18), 4926 (1999).

Hilbi, H.,Modulation of phosphoinositide metabolism by pathogenic bacteria *Cell Microbiol* **8** (11), 1697 (2006).

Hueck, C. J.,Type III protein secretion systems in bacterial pathogens of animals and plants *Microbiol Mol Biol Rev* **62** (2), 379 (1998).

Hume, P. J., McGhie, E. J., Hayward, R. D., and Koronakis, V.,The purified *Shigella* IpaB and *Salmonella* SipB translocators share biochemical properties and membrane topology *Mol Microbiol* **49** (2), 425 (2003).

Kamgang, R., Pouokam, K. E., Fonkoua, M. C., Penlap, N. B., and Biwole, S. M.,Shigella dysenteriae type 1-induced diarrhea in rats *Jpn J Infect Dis* **58** (6), 335 (2005).

Klausser, T., Kramer, J., Otzelberger, K., Pohlner, J., and Meyer, T. F.,Characterization of the *Neisseria* IgA beta core: The essentail unit for outer membrane targeting and extracellular protein secretion *J Mol Biol* **234** (579-593) (1993).

Kotloff, K. L., Winickoff, J. P., Ivanoff, B., Clemens, J. D., Swerdlow, D. L., Sansonetti, P. J., Adak, G. K., and Levine, M. M.,Global burden of Shigella infections: implications for vaccine development and implementation of control strategies *Bull World Health Organ* **77** (8), 651 (1999).

Kueltzo, L. A., Osiecki, J., Barker, J., Picking, W. L., Ersoy, B., Picking, W. D., and Middaugh, C. R.,Structure-function analysis of invasion plasmid antigen C (IpaC) from *Shigella flexneri J Biol Chem* **278** (5), 2792 (2003).

Lafont, F., Tran Van Nhieu, G., Hanada, K., Sansonetti, P., and van der Goot, F. G.,Initial steps of *Shigella* infection depend on the cholesterol/sphingolipid raft-mediated CD44-IpaB interaction *Embo J* **21** (17), 4449 (2002).

Lakowicz, J. R., *Principles of Fluorescence Spectroscopy*. (Plenum Press, New York, 1983).

Lobley, A., Whitmore, L. ,Wallace, B.A,DICHROWEB: an interactive website for the analysis of protein secondary structure from circular dichroism spectra. *Bioinformatics* **18**, 211 (2002).

Mach, H. and Middaugh, C. R.,Interaction of partially structured states of acidic fibroblast growth factor with phospholipid membranes *Biochemistry* **34** (31), 9913 (1995).

Mallett, C., L. VanDeVerg, H.H. Collins, and T. L. Hale,Evaluation of *Shigella* vaccine safety and efficacy in an intranasally challenged mouse model *Vaccine* **11** (2), 190 (1993).

Menard, R., Sansonetti, P. J., and Parsot, C.,Nonpolar mutagenesis of the ipa genes defines IpaB, IpaC, and IpaD as effectors of *Shigella flexneri* entry into epithelial cells *J Bacteriol* **175** (18), 5899 (1993).

Menard, R., Sansonetti, P., and Parsot, C.,The secretion of the *Shigella flexneri* Ipa invasins is activated by epithelial cells and controlled by IpaB and IpaD *Embo J* **13** (22), 5293 (1994).

Menard, R., Sansonetti, P., Parsot, C., and Vasselon, T.,Extracellular association and cytoplasmic partitioning of the IpaB and IpaC invasins of *S. flexneri Cell* **79** (3), 515 (1994).

Menard, R., Prevost, M. C., Gounon, P., Sansonetti, P., and Dehio, C.,The secreted Ipa complex of *Shigella flexneri* promotes entry into mammalian cells *Proc Natl Acad Sci U S A* **93** (3), 1254 (1996).

Mounier, J., Vasselon, T., Hellio, R., Lesourd, M., and Sansonetti, P. J.,Shigella flexneri enters human colonic Caco-2 epithelial cells through the basolateral pole *Infect Immun* **60** (1), 237 (1992).

Mounier, J., Laurent, V., Hall, A., Fort, P., Carlier, M. F., Sansonetti, P. J., and Egile, C.,Rho family GTPases control entry of Shigella flexneri into epithelial cells but not intracellular motility *J Cell Sci* **112 (Pt 13)**, 2069 (1999).

Niebuhr, K., Giuriato, S., Pedron, T., Philpott, D. J., Gaits, F., Sable, J., Sheetz, M. P., Parsot, C., Sansonetti, P. J., and Payrastre, B.,Conversion of PtdIns(4,5)P(2) into PtdIns(5)P by the *S. flexneri* effector IpgD reorganizes host cell morphology *Embo J* **21** (19), 5069 (2002).

Olive, A. J., Kenjale, R., Espina, M., Moore, D. S., Picking, W. L., and Picking, W. D.,Bile salts stimulate recruitment of IpaB to the Shigella flexneri surface, where it colocalizes with IpaD at the tip of the type III secretion needle *Infect Immun* **75** (5), 2626 (2007).

Page, A. L., Ohayon, H., Sansonetti, P. J., and Parsot, C.,The secreted IpaB and IpaC invasins and their cytoplasmic chaperone IpgC are required for intercellular dissemination of *Shigella flexneri Cell Microbiol* **1** (2), 183 (1999).

Page, A. L., Fromont-Racine, M., Sansonetti, P., Legrain, P., and Parsot, C.,Characterization of the interaction partners of secreted proteins and chaperones of Shigella flexneri *Mol Microbiol* **42** (4), 1133 (2001).

Parsot, C., Menard, R., Gounon, P., and Sansonetti, P. J.,Enhanced secretion through the Shigella flexneri Mxi-Spa translocon leads to assembly of extracellular proteins into macromolecular structures *Mol Microbiol* **16** (2), 291 (1995).

Phalipon, A. and Sansonetti, P. J.,Shigella's ways of manipulating the host intestinal innate and adaptive immune system: a tool box for survival? *Immunology and cell biology* **85** (2), 119 (2007).

Picking, W. L., Coye, L., Osiecki, J. C., Barnoski Serfis, A., Schaper, E., and Picking, W. D.,Identification of functional regions within invasion plasmid antigen C (IpaC) of *Shigella flexneri Mol Microbiol* **39** (1), 100 (2001).

Picking, W. L., Nishioka, H., Hearn, P. D., Baxter, M. A., Harrington, A. T., Blocker, A., and Picking, W. D. IpaD of *Shigella flexneri* is independently required for regulation of Ipa protein secretion and efficient insertion of IpaB and IpaC into host membranes *Infect Immun* **73** (3), 1432 (2005).

Pukatzki, S., Ma, A.T., Sturtevant, D., Krastins, B., Sarracino, D., Nelson, W.C., *et al.* Identification of a conserved bacterial protein secretion system in *Vibrio cholerae* using the *Dictyostelium* host model system. *Proc Natl Acad Sci USA* **103,** 1528 (2006).

Russel, M.,Macromolecular assembly and secretion across the bacterial cell envelope: Type II protein secretion systems *J Mol Biol* **279**, 485 (1998).

Sansonetti, P. J., Kopecko, D. J., and Formal, S. B.,*Shigella sonnei* plasmids: evidence that a large plasmid is necessary for virulence *Infect Immun* **34** (1), 75 (1981).

Sansonetti, P. J., d'Hauteville, H., Formal, S. B., and Toucas, M.,Plasmid-mediated invasiveness of "Shigella-like" Escherichia coli *Ann Microbiol (Paris)* **133** (3), 351 (1982).

Sansonetti, P. J., Kopecko, D. J., and Formal, S. B.,Involvement of a plasmid in the invasive ability of *Shigella flexneri Infect Immun* **35** (3), 852 (1982).

Sansonetti, P. J., Arondel, J., Cantey, R., Prevost, M.C., and Huerre, M..Infection of rabbit Peyer's patches by *Shigella flexneri*: effect of adhesive or invasive bacterial phenotypes on follicle-associated epithelium. *Infect Immun* **64** (7), 2752 (1996).

Schroeder, G. N. and Hilbi, H.,Molecular pathogenesis of Shigella spp.: controlling host cell signaling, invasion, and death by type III secretion *Clin Microbiol Rev* **21** (1), 134 (2008).

Schnell, D. J. and Herbert, D. N.,Protein translocons: Multifunctional mediators of protein translocation across membranes *Cell* **112** (4), 491 (2003).

Shiga, K. 1897. Sekiri byogen kenkyu hokoku dai-ichi (first report on etiologic research on dysentery). *Saikingaku Zasshi* **25** (1),790 (1897).

Stender, S., Friebel, A., Linder, S., Rohde, M., Mirold, S., and Hardt, W. D.,Identification of SopE2 from Salmonella typhimurium, a conserved guanine nucleotide exchange factor for Cdc42 of the host cell *Mol Microbiol* **36** (6), 1206 (2000).

Tran Van Nhieu, G., Caron, E., Hall, A., and Sansonetti, P. J.,IpaC induces actin polymerization and filopodia formation during *Shigella* entry into epithelial cells *Embo J* **18** (12), 3249 (1999).

van der Goot, F. G., Tran van Nhieu, G., Allaoui, A., Sansonetti, P., and Lafont, F.,Rafts can trigger contact-mediated secretion of bacterial effectors via a lipid-based mechanism *J Biol Chem* **279** (46), 47792 (2004).

Wassef, J.S., Keren, D.F., and Mailloux, J.L..Role of M cells in initial antigen uptake and in ulcer formation in the rabbit intestinal loop model of shigellosis *Infect Immun* **57** (3), 858 (1989).

Watarai, M., Tobe, T., Yoshikawa, M., and Sasakawa, C.,Contact of Shigella with host cells triggers release of Ipa invasins and is an essential function of invasiveness *Embo J* **14** (11), 2461 (1995).

Winans, S. C., Burns, D. L., and Christie, P. J.,Adaptation of a conjugal transfer system for the export of pathogenic molecules *Trends Microbiol* **4**, 64 (1996).

Yoshikawa, M., Sasakawa, C., Makino, S., Okada, N., Lett, M. C., Sakai, T., Yamada, M., Komatsu, K., Kamata, K., Kurata, T., and *et al.*,Molecular genetic approaches to the pathogenesis of bacillary dysentery *Microbiol Sci* **5** (11), 333 (1988).

Zheng, J., Leung, K.Y. Dissection of a type VI secretion system in Edwardsiella tarda *Mol Microbiol* **66** (5), 1192 (2007).

Zychlinsky, A., Kenny, B., Menard, R., Prevost, M. C., Holland, I. B., and Sansonetti, P. J.,IpaB mediates macrophage apoptosis induced by *Shigella flexneri Mol Microbiol* **11** (4), 619 (1994).